Non-human primate models of human respiratory infections

Julien Lemaitre [a,1], Thibaut Naninck [a,1], Benoît Delache [a], Justina Creppy [a,b], Philippe Huber [a], Marion Holzapfel [a], Camille Bouillier [a], Vanessa Contreras [a], Frédéric Martinon [a], Nidhal Kahlaoui [a], Quentin Pascal [a], Sabine Tricot [a], Frédéric Ducancel [a], Laurent Vecellio [b,c], Roger Le Grand [a], Pauline Maisonnasse [a,*]

[a] Université Paris-Saclay, INSERM, CEA, Center for Immunology of Viral, Autoimmune, Hematological and Bacterial Diseases (IMVA-HB/IDMIT), Fontenay-aux-Roses & Le Kremlin-Bicêtre, France
[b] Centre d'Etude des Pathologies Respiratoires, INSERM U1100, Université de Tours, Tours, France
[c] Plateforme Scientifique et Technique Animaleries (PST-A), Université de Tours, Tours, France

ABSTRACT

Respiratory pathogens represent a great burden for humanity and a potential source of new pandemics, as illustrated by the recent emergence of coronavirus disease 2019 (COVID-19). In recent decades, biotechnological advances have led to the development of numerous innovative therapeutic molecules and vaccine immunogens. However, we still lack effective treatments and vaccines against many respiratory pathogens. More than ever, there is a need for a fast, predictive, preclinical pipeline, to keep pace with emerging diseases. Animal models are key for the preclinical development of disease management strategies. The predictive value of these models depends on their ability to reproduce the features of the human disease, the mode of transmission of the infectious agent and the availability of technologies for monitoring infection. This review focuses on the use of non-human primates as relevant preclinical models for the development of prevention and treatment for human respiratory infections.

1. Introduction

Lower respiratory tract infections (LRTI) are the fourth leading cause of death worldwide, and tuberculosis and acute LRTI are the two most common causes of severe illness and death (WHO, 2020). Respiratory pathogens have been extensively studied in various animal models, leading to the development of a number of effective vaccines and treatments. Common pathogens, such as influenza viruses, continue to circulate in human populations and between animals and humans, resulting in yearly epidemic waves in the absence of broadly protective ("universal") vaccines. The recent coronavirus outbreak has highlighted the need for improvements in our understanding of the immune system of the respiratory tract (RT), to facilitate the development of vaccines and treatments for immune disorders associated with severe acute respiratory distress. More than ever, we need to accelerate the development of new preventive or therapeutic strategies, and animal models are key to tackle this challenge. Mouse models have many advantages, as mice reproduce rapidly and require limited resources in experimental

settings, even if high levels of biosafety containment are required. Furthermore, many tools are available for exploring their immune functions and pathogenesis. These models are, thus, highly valuable for improving our understanding of the basic molecular and cellular mechanisms of host/pathogen interactions. However, they are also subject to a number of limitations for studies of human infections and of the countermeasures envisaged (Masopust et al., 2017). Mice are phylogenetically distant from humans and often lack the appropriate receptors for the entry and dissemination of human pathogens. The mechanisms of innate and adaptive immunity also differ significantly between mice and humans. Syrian hamsters and ferrets (Gretebeck and Subbarao, 2015; van den Brand et al., 2014) are frequently used as models for respiratory infections because the mode of transmission of the infectious agent and the resulting pathogenesis in these animals more closely resemble the features of human respiratory infections. However, very few tools are available for exploring the host factors associated with disease susceptibility in these animals, or for characterizing the immune effectors underlying protective immunity. In many

respects, non-human primates (NHPs) appear to constitute a particularly relevant preclinical model for respiratory infectious diseases, because pathogenesis in NHPs more closely resembles that in human patients, and because treatments found to be effective in NHPs can more easily be translated into clinical practice for humans (Bluemel, 2015). Apes, and chimpanzees in particular, were historically used as research models for studies of infectious diseases. However, for ethical and conservation reasons, their use is no longer permitted in many countries, or they must be used only in strictly controlled studies confined to a very small number of research areas in which no alternative is available (NEAVS, 2021; NIH, 2015). Most of the biomedical research performed on NHPs these days involves species such as macaques, baboons, marmosets, and African green monkeys (AGM). The use of NHPs for research purposes requires highly specific facilities and specialized staff. Despite the high cost of studies in NHPs, these animals are still widely used in studies of pathogenesis, preclinical studies of prophylaxis, and treatment trials. In this review, we summarize the key features of NHP use for translational research on human respiratory infections. Below, we address the comparative anatomy, physiology and immunology of NHPs relative to humans, and the contribution of NHP studies to improving our understanding of the pathophysiology of respiratory infections. We then focus on new technologies that will improve this preclinical model for both the modeling of pathogen exposure and the development of *in vivo* imaging.

2. Comparative anatomy and physiology of the respiratory tracts of non-human primates and humans

We will first present a short description of the anatomy and physiology of NHP airways, comparing them to those of humans, and will then focus on the principal immunological features for investigation in pathophysiological studies, as described by Miller et al. (2017).

2.1. Anatomy of the airways and lungs

The RT is divided into the upper respiratory tract (URT; the nose, nasal cavity, pharynx) and the lower respiratory tract (LRT; larynx, trachea, bronchi and lungs). The structure and organization of the airways (trachea and bronchi) are probably the source of the largest differences in RT anatomy between mammals. More detailed reviews on comparative RT anatomy between mammals are available elsewhere (Patra, 1986). NHPs are the mammalian species used in research with the most similar airway anatomy to humans (Harkema, 1991). Both humans and NHP species breathe *via* both the nose and mouth, whereas rodents breathe *via* the nose only. Both humans and NHPs have far fewer, more basic turbinates in the nasal cavity than rodents, carnivores and pigs, indicating a relatively similar spatial distribution of epithelial cells (Harkema, 1991; Parent, 2015). In addition, the segmentation of the tracheobronchial tree in humans and NHPs is also similar, with a dichotomous airway organization, contrasting with the monopodial anatomy observed in rodents and pigs (Judge et al., 2014; Parent, 2015). This organization delineates a clear separation between the lung lobes, with laboratory NHPs having lungs consisting of two left lobes and four right lobes (Plopper and Harkema, 2005). The right accessory lobe of these animals is not present in humans and great apes, and constitutes the major difference between these groups. The bronchus of NHPs, like that of humans, separates into several intrapulmonary bronchi, followed by terminal bronchioles, leading to the acini (Parent, 2015; Patra, 1986). There are several histological similarities between NHPs and humans. In both, the cartilage extends to the proximal intrapulmonary bronchus, and smooth muscles remain abundant until the terminal bronchioles (Parent, 2015). This feature plays an important role in acute and chronic lung infections, regulating airway caliber and ventilation in response to inflammation. Mucosal ciliate cells and club cells, and the intraepithelial distribution of nerves in the bronchus are also similar in NHPs and humans, suggesting a similar mode of operation of the mucociliary escalator (Castleman et al., 1975). Thus, the anatomy and

histology of the RT of NHPs closely resemble those of humans, making NHPs unique models in terms of both lesion organization and the local response to pathogens.

2.2. Physiology of the respiratory tract

The physiology of the respiratory tract also affects the pathophysiological processes occurring during respiratory infections, and has been studied in detail in NHPs. Evaluations of respiratory system function, based on respiratory patterns, rate, tidal volume, and other parameters, have been extensively used in NHPs for drug testing (Bluemel, 2015). Minute ventilation (*i.e.* the product of tidal volume and respiratory rate), the inspiratory/expiratory time ratio and mean inspiratory flow (tidal volume/inspiratory time) are important parameters characterizing the stimulation or depression of the respiratory system, and airway obstruction (Remmers, 1976). In addition to these ventilator parameters, airway patency and elastic recoil of the lung can be evaluated in NHPs by measuring airway resistance and lung compliance, respectively. Indeed, several underlying pathophysiological mechanisms may alter lung compliance and airway resistance, which is particularly high in cases of bronchoconstriction, edema, or epithelial hyperplasia (Hogg, 2004).

Several technical approaches have been developed for evaluating respiratory parameters in anesthetized and conscious NHPs, as extensively reviewed elsewhere (Bluemel, 2015). The relevance of these approaches, which were initially developed for drug evaluation, in translational research lies in the use of methods similar to those developed in clinical settings. Plethysmography is widely used for the evaluation of lung function in patients, providing data for various parameters, including residual volume, airway resistance and total lung capacity (Criée et al., 2011). Head-out plethysmography has been adapted for use in BSL3 laboratories, making it possible to explore the impact of *Yersinia pestis* or *Mycobacterium tuberculosis* (*Mtb*) infections in macaques (Obot Akata et al., 2007; Sharpe et al., 2017). Forced oscillometry has been used in conscious and anesthetized cynomolgus macaques (CM) (Bassett et al., 2014). This non-invasive approach has been successfully used in humans, for obstructive lung diseases (Ram et al., 2019). This technology provides a good example of the tools available for NHP studies, making this animal model an excellent choice for drug safety assessments and for exploring the role of small airways in respiratory infections.

3. Key immune effectors in the NHP lung

The anatomy and physiology of the respiratory tract must be taken into account when designing the exposure model and monitoring the clinical symptoms occurring during the course of respiratory infection. However, the key parameters in pathophysiological studies are those of the immune system. Indeed, the RT is continually exposed to aerosols, particles, microbiota, and invading pathogens.

The immune system operates in strategic areas, and local lymphoid tissues are associated with the mucosae (nasopharynx-associated lymphoid tissue or NALT, bronchus-associated lymphoid tissue or BALT) and distant sites, such as the cervical and mediastinal lymph nodes. NALT and BALT are mucosa-associated lymphoid tissues (MALT) and can be classified on the basis of function as inductive and effector sites. Inductive sites consist of secondary lymphoid tissue (follicles and T-cell zones), whereas effector sites consist of immune cells (mostly CD4^{+} T cells, IgA-producing plasma cells, dendritic cells (DC) and macrophages) disseminated across the mucosae (Cesta, 2006). NALT displays a similar organization in humans and NHPs. The NALT inductive sites consist of Waldeyer's rings: two tonsil palatines, two tubal tonsils, adenoid and lingual tonsils (Casadei and Salinas, 2019). Tonsils are secondary lymphoid organs covered by an epithelium, forming cryptic structures and containing follicles, M cells, lymphocytes, DC, macrophages, and some neutrophils. Rodents lack Waldeyer's rings and have NALT only in

the caudoventral portions of the nasal cavities, at the entrance to the nasopharyngeal duct (Casadei and Salinas, 2019). These structures in the nasal cavities are also present in NHPs and humans. BALT also varies considerably between species, being absent from dogs, cats and Syrian hamsters. In humans and NHPs, BALT is randomly distributed in the bronchial airways, and preferentially localized at the bronchial tree bifurcation (Cesta, 2006).

NHPs are, thus, the closest species to human in terms of lung structure and physiology, but also in terms of immune system localization and composition. As explained below, this close resemblance also translates into similar susceptibilities to respiratory pathogens and similar pathophysiological features in cases of infection.

4. Role of NHPs in the modeling of respiratory tract infections

Not only do NHPs display anatomical, physiological and immunological similarities to humans, but they also present similar symptoms to humans when infected with various pathogens. Some of the findings detailed in the following paragraphs have been reviewed elsewhere (Miller et al. (2017)) but advances necessitate an update, particularly for coronaviruses.

4.1. Influenza viruses

Influenza or flu is a contagious respiratory disease caused by members of the *Orthomyxoviridae* family. It may be seasonal, with severe cases occurring mostly in children < 5 years old, pregnant women and adults > 65 years old (Thompson et al., 2003), or pandemic, as in the 1918 and 2009 pandemics caused by H1N1 strains and resulting in unusually high mortality rates among young people (Simonsen et al., 1998; Van Kerkhove et al., 2013). Highly pathogenic H5N1 avian strains with high mortality rates have also been emerging since 2003 (WHO, 2018a).

Uncomplicated influenza is characterized by an acute onset of URT signs and symptoms, such as fever, myalgia, headache, lethargy, anorexia, non-productive cough, sore throat, and rhinitis, lasting for one to two weeks. In elderly or fragile patients, pulmonary complications may occur, including primary viral pneumonia and secondary bacterial pneumonia, acute respiratory distress syndrome (ARDS), shock, and even death (CDC, 2019). Infections with avian strains, such as the H5N1, can cause similarly severe symptoms in young, healthy patients. Gastrointestinal symptoms and conjunctivitis have been reported in H5N1 and H7 infections, respectively (WHO, 2018a; Yu et al., 2008). Antibodies are generated against various viral proteins, but mostly against HA and NA, both of which are subject to antigenic drift and antigenic shift. CD8$^+$ effector T-cell responses are directed principally against the most conserved proteins, *i.e.* the NP, M and P1 proteins (Boon et al., 2002; Wang et al., 2007), but viral escape may nevertheless occur (Berkhoff et al., 2007).

A new vaccine is formulated each year, in accordance with WHO recommendations. It contains the four strains considered to be the most likely to circulate in the year concerned. These vaccines can provide 70–90% protection against symptoms caused by the vaccine strains, but a "universal vaccine" with broad protective efficacy would be required to improve the control of emerging seasonal variants. Antiviral treatments are available, but with a narrow window of use (Shie and Fang, 2019).

Small-animal models are widely used to study influenza viruses. Ferrets, guinea pigs, hamsters and cotton rats are naturally susceptible to infection with human influenza virus strains. Other species, such as mice, can be infected only after adaptation of the human virus. However, influenza disease in these species is clinically unapparent, and symptoms cannot, therefore, be used to assess the progression of infection or disease control with antiviral drugs or vaccines in preclinical trials (Bouvier and Lowen, 2010).

Non-human primates are susceptible to infection with a number of human influenza A isolates, including viruses of the H3N2, H5N1 and H1N1 subtypes (Bouvier and Lowen, 2010). Some studies have also highlighted the susceptibility of CM to influenza B strains (Davis et al., 2015; Kitano et al., 2010, 2011). The first reports of naturally occurring infections in wild or captive monkeys emerged in 1919 (Davis et al., 2015). In experimental settings, all the tested species shed the virus and almost all developed symptoms. Various species have since been used for trials of vaccination and antiviral drugs. Most of these studies were performed on RM and CM, but some studies have also been performed on baboons (Heberling and Kalter, 1970), squirrel monkeys (Scott et al., 1978; Stephen et al., 1977) and pig-tailed macaques (Baskin et al., 2007; Jegaskanda et al., 2013).

As in humans, the infection of RM and CM is characterized by a biphasic fever and various symptoms, depending on the route of experimental exposure, strain and dose; these species are, therefore, highly suitable for use in drug and vaccine evaluation (Arikata et al., 2012; Davis et al., 2015; Margine and Krammer, 2014). RM and CM may display viral shedding in both the URT and the LRT, the depletion of alveolar macrophages, severe symptoms of ARDS (Wonderlich et al., 2017), bronchointerstitial pneumonia, peribronchiolar alveolitis, edema, and hemorrhage (Cillóniz et al., 2009), due to widespread alveolar epithelial cell death (Watanabe et al., 2018).

The importance of the challenge route has been clearly demonstrated. In RM, infection has never been successfully established *via* the IN instillation of influenza virus, but aerosol or IT delivery causes infection, with clinical symptoms (including listlessness and lethargy, facial flushing, and conjunctival injection), leukopenia (Berendt, 1974) and seroconversion, resulting in protection against repeated challenge (Saslaw et al., 1946). It has been suggested that symptom variability is related to strain virulence. The use of combinations of the IN and IT routes, frequently associated with the ocular and conjunctival routes, has become the norm (Davis et al., 2015). Recent studies have also shown that aerosols of H5N1 or H1H1 induce fewer symptoms and weaker immune responses than combined IN + IT exposure in CM (Mooij et al., 2020, 2021).

Thus, the long history of influenza studies in NHPs reflects the changes over time in the species used in laboratories, and in the exposure techniques used for airborne pathogens in studies performed *in vivo*.

4.2. Coronaviruses

Coronaviruses constitute another vast family of respiratory viruses that have been studied for decades. They were identified as responsible for common colds in humans in the 1960s (McIntosh et al., 1967) and have become a matter of major concern since the SARS (severe acute respiratory syndrome) and MERS (Middle East respiratory syndrome) coronavirus outbreaks in 2002 and 2012, respectively, and the emergence of SARS-CoV-2 at the end of 2019.

An estimated 90 % of adults have serum antibodies against HCoV-229E, HCoV−OC43, HCoV-NL63, and HCoV-HKU1 (Gorse et al., 2010; McIntosh and Perlman, 2015), which are thought to be responsible for ~15 % of common colds (Fouchier et al., 2004; van der Hoek et al., 2004; Woo et al., 2005). By early 2021, SARS-CoV-2 had already infected over 100,000,000 people, with an estimated mortality of ~2 %, contrasting with SARS-CoV and MERS-CoV, the circulation of which was limited during their respective outbreaks, as indicated by the number of cases (~8100 and 2,500, respectively), although they were associated with higher mortality (~10 and ~35 %, respectively) (Peiris et al., 2004; WHO, 2021; Zaki et al., 2012).

The common cold-associated strains induce only mild symptoms, and replicate in the nasopharynx. The SARS and MERS viruses were found to replicate in the LRT, inducing severe pneumonia, which can progress to ARDS (Arabi et al., 2017; Gu and Korteweg, 2007; Puelles et al., 2020). Immunopathology, rather than excessive viral replication, appears to underlie severe clinical progression (Peiris et al., 2003). Antibody titers have been shown to wane rapidly for common cold

strains and to be inversely correlated with disease severity for SARS- and MERS-CoV. By contrast, cellular immunity appears to last longer for SARS- and MERS-CoV (Sariol and Perlman, 2020). Other characteristic traits of SARS and COVID-19 include the infiltration of lymphocytes, neutrophils and macrophages into the alveoli and interstitium, epithelial denudation (Nicholls et al., 2003; Zhou et al., 2020), vasculitis, lymphopenia, spleen and lymph node atrophy, and the presence of the virus in the brain, spleen, and other tissues (Gu and Korteweg, 2007; Puelles et al., 2020). There is also growing evidence of extrapulmonary manifestations in COVID-19 patients, including thrombotic complications, acute kidney injury, hepatocellular injury and myocardial dysfunction (Gupta et al., 2020).

Small-animal models have been used to study coronaviruses, but this approach has major limitations (Muñoz-Fontela et al., 2020). Mice are susceptible to infection with SARS-CoV, but they do not display symptoms similar to those in humans (Roberts et al., 2005). For infection with SARS-CoV-1 (McCray et al., 2007; Tseng et al., 2007), SARS-CoV-2 (Bao et al., 2020; Sun et al., 2020) or MERS (Cockrell et al., 2016; Li et al., 2017; Zhao et al., 2014), they must be humanized or infected with adapted strains (Roberts et al., 2007). MERS can replicate in the lungs of rabbits, which may display seroconversion, but with no symptoms or manifestations of disease (Haagmans et al., 2015). Ferrets and Syrian hamsters are highly susceptible to SARS-CoV-2 infection and are able to transmit SARS-CoV-2 to other animals in the same housing, but ferrets have low viral titers and few symptoms (Kim et al., 2020; Shi et al., 2020), and older male hamsters have higher viral titers, slight weight loss, moderate-to-severe lung disease and more severe symptoms (Chan et al., 2020; Imai et al., 2020; Sia et al., 2020).

Common marmosets can be used as models for MERS and SARS, but they appear to be relatively resistant to SARS-CoV-2 infection. They develop lethal pneumonia following intratracheal (IT) exposure to MERS-CoV, and this led to their use as models for drug evaluation (Chan et al., 2015). A few studies have reported SARS and SARS-CoV-2 infection in marmosets exposed *via* the IT and/or IN routes (Lu et al., 2020). All SARS-infected animals presented lesions, with viral RNA and inflammatory changes detected in the lung. Only one third of the marmosets exposed to SARS-CoV-2 developed fever; viral RNA was detected until day 14 in nasal, tracheal, and rectal swabs, and in blood. However, no pneumonia was observed, no viral RNA was detected in other tissues, and there was no seroconversion (Lu et al., 2020).

Both SARS-CoV-1 and -2 can replicated in the URT and LRT of AGMs, with similar results obtained for both viruses (Cross et al., 2020; Hartman et al., 2020; McAuliffe et al., 2004; Woolsey et al., 2021). Lower replication rates and milder lung disease were observed after exposure *via* the IN route only than after the use of a combination of the IN and IT routes (Cross et al., 2020; Woolsey et al., 2021). The monkeys developed only mild clinical signs, if any, but presented signs of coagulopathy, high liver enzyme levels, focal interstitial mononuclear infiltration in the lungs, edema and macrophage infiltration. They rapidly developed antibody responses that protected against rechallenge with the same strain (McAuliffe et al., 2004; Woolsey et al., 2021).

Baboons were recently used in SARS-CoV-2 studies of age-related susceptibility and in vaccination studies (Singh et al., 2021; Tian et al., 2021). The virus replicates in the URT and LRT of these animals, with prolonged viral RNA shedding. Old animals displayed stronger lung inflammation than young animals, and significantly stronger inflammation was observed in baboons than in RM, regardless of the age of the animals studied (Singh et al., 2021).

RM and CM are the most frequently used NHP models studies of for coronavirus disease and for the preclinical evaluation of therapeutic agents (Maisonnasse et al., 2020; Williamson et al., 2020) and vaccines (Brouwer et al., 2021; Corbett et al., 2020). CM and RM were the first animal models used for studies of SARS (Fouchier et al., 2003) and MERS (Munster et al., 2013), respectively. The doses of inoculum and routes of inoculation are similar in all studies for all viruses, ranging from 10^5 to 10^7 PFU/animal, mostly delivered *via* a combination of the

IN and IT routes, and sometimes also *via* the oral and ocular routes.

RM exposed to MERS presented temporary, mild-to-moderate clinical signs, viral RNA in the RT, infiltrations and interstitial labeling with inflammatory markers, and on chest X-rays, during the first few days of infection. Neutralizing antibodies (NAbs) were detected as early as 7 dpi (De Wit et al., 2013; Munster et al., 2013; Yao et al., 2014). Similar results were obtained for SARS-infected CM (Kuiken et al., 2003; Osterhaus et al., 2004).

When infected with SARS-CoV-2 *via* the IN and/or IT routes, both CM and RM present mild-to-moderate symptoms. Viral RNA is detectable throughout the respiratory and gastrointestinal tract, and in other organs (Chandrashekar et al., 2020; Deng et al., 2020a; Lu et al., 2020; Munster et al., 2020; Shan et al., 2020), mimicking the infection observed in most humans without comorbidity. The hallmarks of human SARS-CoV-2 infection — pulmonary edema and diffuse interstitial pneumonia — were observed on X-rays during these studies. In comparative studies, old RM and CM suffered from more severe interstitial pneumonia, with higher viral loads in the lungs and on rectal swabs, and viral replication throughout the lung (Rockx et al., 2020). By contrast, only the upper lobes of the lung appeared to be affected in younger RM (Yu et al., 2020). Old RM also developed higher antibody levels (Lu et al., 2020). However, no mortality was observed, even in the geriatric groups (Rockx et al., 2020), contrasting with the severe systemic responses observed in older macaques with SARS (Smits et al., 2010). Upon reinfection, shortly after a first exposure, viral loads in the RM were lower, according to analyses of BAL, nasopharyngeal swabs, and rectal swabs, and no symptoms were observed (Chandrashekar et al., 2020).

Various anti-SARS-CoV-2 vaccines have already been tested in RM and CM, and have been shown to decrease genomic and subgenomic RNA levels in nasal and/or tracheal swabs. In all studies, the animals developed NAbs. Only one of these studies showed an increase in IgA levels in the mucosal fluids (Brouwer et al., 2021). This finding is of particular importance, given that mucosal antibodies appear to be the most relevant for establishing the likelihood of reinfection (Habibi et al., 2015; Singleton et al., 2003). Indeed, preclinical studies for SARS and MERS highlighted the importance of IgA-driven immune responses and of the localization of T cells to the RT, and vaccine candidates have been shown to yield higher levels of protection following IN immunization than after immunization *via* parenteral routes (Jia et al., 2019; Kim et al., 2019; Zhao et al., 2016).

A vaccine-associated enhancement of respiratory disease (VAERD) has been observed in vaccine trials performed on animal models of SARS, including NHPs (Liu et al., 2019), and in mice immunized against a human SARS-CoV isolate and challenged with a heterologous strain of the virus (Deming et al., 2006).

Like influenza viruses, coronaviruses have been studied in various NHP species. However, these viruses elicited little research interest until the turn of the century, and research on coronaviruses has built largely on previously acquired knowledge for influenza viruses. Age has also been studied as a risk factor in NHPs infected with coronaviruses, as a means of reproducing the risk factor associated with some comorbidities in humans, but it did not seem to be associated with more severe disease in SARS-CoV-2-infected NHPs. Other techniques will probably be required to obtain a model of severe disease.

4.3. Respiratory syncytial virus

Human respiratory syncytial virus (hRSV) is another highly contagious virus that can provoke acute respiratory illnesses. In healthy adults, hRSV infection resembles the common cold (Hall et al., 2001), but in infants, it is the principal cause of acute bronchiolitis (Shi et al., 2017) and is associated with hospitalization and mortality rates similar to those of influenza in elderly and fragile adults (Falsey et al., 2005; Lee et al., 2013; Widmer et al., 2012). Its prevalence is extremely high: 70 % of children are infected in their first year of life, and more than 99 % are

infected within the first two years (Glezen, 1986). Reinfections occur throughout life, at a rate of 5–10 % per year (Falsey et al., 2005).

Unfortunately, despite more than 60 years of research, only a few vaccines and curative treatments been developed to the phase 3 clinical testing stage, and none has been approved for market release (Thornhill et al., 2020). Prophylaxis with the monoclonal palivizumab antibody (Synagis®) can decrease the risk of hospitalization by 50 % (Andabaka et al., 2013). However, this strategy is very costly and is, thus, recommended only for infants at high risk (premature or with certain cardiac or pulmonary conditions) (Wang et al., 2008). In this context, *in vivo* infection models are crucial for understanding hRSV pathogenesis and characterizing disease-associated and protective immune responses. Many animal models exist, but most display limited viral replication, with few symptoms and the development of URTI in some cases, but not of LRTI (Altamirano-Lagos et al., 2019; Bem et al., 2011; Taylor, 2017).

Mice, cotton rats, ferrets and neonatal lambs are semi-permissive to hRSV infection, display some clinical symptoms and can develop LRTI (Boukhvalova et al., 2009; Larios Mora et al., 2015; Gregory A. Prince et al., 1978; Stark et al., 2002; Stittelaar et al., 2016). However, the differences between their immune systems and RT structures and those of humans, and the limited availability of molecular tools limit the use of these models.

Several NHP species have been used as models of RSV infection. Chimpanzees are naturally susceptible to hRSV infection. Indeed, the virus was first isolated from a colony of chimpanzees with clinical signs of URTI (Morris et al., 1956) similar those observed in humans (Belshe et al., 1977). No LRTI has been observed in experimentally infected chimpanzees, but a few fatal cases of hRSV-associated bronchopneumonia have been reported in naturally infected chimpanzees displaying the histopathological alterations characteristic of acute LRTI (Clarke et al., 1994; Szentiks et al., 2009).

African green monkeys, owl monkeys, cebus monkeys, CM, RM and bonnet macaques can be experimentally infected with hRSV, but only at high doses (10^5 to 10^8 PFU), and with moderate rates of viral replication. Unlike macaques, African green monkeys, owl monkeys and cebus monkeys may present clinical signs, such as rhinorrhea, conjunctivitis, sneezing and wheezing. Following IT inoculation, AGM, owl monkeys and macaques develop only mild interstitial pneumonia, whereas cebus monkeys present gross pneumonic lesions in the lung (Babu et al., 1998; de Swart et al., 2002; Kakuk et al., 1993; McArthur-Vaughan and Gershwin, 2002; Prince et al., 1979; Richardson et al., 1978; Simoes et al., 1999; Weltzin et al., 1996).

Infant baboons have also been infected with hRSV intratracheally, leading to clinical signs of LRTI and major histopathological changes. However, the decrease in viral titers observed in BAL after 24 h suggests that the damage to the lungs may be due to a non-specific inflammatory response to high-dose inoculation, rather than viral replication (Papin et al., 2013).

NHP models have been used to study the mechanisms of vaccine-enhanced RSV disease (de Swart et al., 2002; Kakuk et al., 1993; Ponnuraj et al., 2001). This phenomenon has been a major concern in vaccine development since its discovery in the 1960s, when the vaccination of children with a formaldehyde-inactivated virus led to 80 % hospitalization, with two deaths upon subsequent infection (Kim et al., 1969). Studies confirmed that a skewing of the T-cell response towards Th2 cytokines was the major cause of this vaccine-enhanced disease and suggested that sensitization to cell culture components present in the vaccine might also have played a role.

Early vaccines were often tested on chimpanzees (Collins et al., 1990; Crowe et al., 1993; Teng et al., 2000), but RM and AGM are now the species most widely used for preclinical studies of RSV vaccination, followed by CM (Bates et al., 2016; Correia et al., 2014; Grunwald et al., 2014; Jones et al., 2012; Marcandalli et al., 2019; Patton et al., 2015; Sesterhenn et al., 2020).

This virus has, thus, been studied *in vivo* for decades, and various limitations have been encountered in most of the NHP species tested, in terms of symptoms or viremia relative to those observed in humans. Nevertheless, NHPs remain the best preclinical model, due to their immunological and physiological closeness to humans. Similar questions about the most appropriate species and exposure techniques for infection have also been posed for airborne bacteria, as described below.

4.4. Tuberculosis

Tuberculosis (TB) is the most important infectious disease worldwide. It is caused by a single pathogen, Mtb. This highly contagious bacterial disease is transmitted between humans *via* the inhalation of aerosolized infected droplets. Of the 30 % of individuals infected, only 5–10% develop clinical manifestations of active TB. The vast majority of infected individuals present only latent TB. Tuberculosis principally affects the lungs and exists as a continuous spectrum of disease states, from dormant to fulminant infection (Lin and Flynn, 2018). We still know little about the transition from latent to active TB. The classic symptoms are non-specific and include weight loss, the coughing up of blood-containing mucus and a wide range of other symptoms, depending on the other organs affected. The hallmark of the disease is the development of granulomas, organized aggregates of macrophages and lymphocytes, the nature of which may vary considerably within and between individuals (Scanga and Flynn, 2014). TB diagnosis remains difficult and is based principally on immunological tests (tuberculin skin test (TST), interferon gamma release assay (IGRA)), and chest X-rays. A major resurgence of TB has occurred in recent decades, associated with the global failure of anti-TB vaccination with BCG (*Mycobacterium bovis* Bacillus Calmette–Guerin). BCG continues to protect children against active tuberculosis but is ineffective against pulmonary forms in adults. The impact of the disease has also been increased by HIV co-infection, and the progression of drug-resistant Mtb, including multidrug-resistant bacteria (WHO, 2020). Novel therapeutic strategies are required to control the TB pandemic, and international efforts have intensified in recent decades, through initiatives such as the WHO End TB Strategy, which aims to decrease TB-related mortality by 90 % by 2030 (WHO, 2020).

Several animal models, including guinea pig, rabbit, mouse and zebrafish, have been used to study the basic pathogenesis of TB, but none of these models fully reproduces the full range of disease stages and the diversity of pathological lesions. NHP models, especially macaques, have been used to study TB since the 1960s (Kaushal et al., 2012). These animals are the preferred models because they provide the best reproduction of the full spectrum of human disease and infection outcomes. Moreover, they respond to many human drug agents in a similar manner to humans, they can be monitored with identical parameters, and they present variable responses to BCG vaccination, as reported for humans (Flynn et al., 2015; Peña and Ho, 2015). They have, therefore, been widely used in immunological studies, studies of pathogenesis, and vaccine development. A common marmoset model of TB has recently been developed. Marmosets have the advantage of being much smaller than other NHP species, and they can be used for dizygotic twin comparisons. They are also highly susceptible to diverse Mtb strains. The technologies used with macaques can also be applied to marmosets, providing opportunities for testing new drug regimens using smaller doses of antibiotics (Cadena et al., 2016; Via et al., 2013). The principal limitation to the use of marmoset models is the lack of tools for exploring immune responses and absence of a latent form of TB.

The form of TB disease and its progression in NHPs depend on several parameters, including Mtb strain (CDC1551, Erdman, H37RV, Beijing isolate), the dose of inoculum — very low (1–10 CFU), low (10–50 CFU), medium (< 500 CFU), high or very high (> 1400 CFU) — and the route of infection (intranasal (IN), intrabronchial (IB) or IT instillation, aerosol route, intravenously) (Cadena et al., 2016). NHP species and geographic origin also affect disease progression. For example, RM are more susceptible to Mtb infection and are better models of active TB than CM, which are mostly used to study latent disease (Capuano 3rd

et al., 2003; Dijkman et al., 2019; Maiello et al., 2018; Sharpe et al., 2016). Moreover, CM originating from Asia (high levels of genetic diversity) appear to be more able to control the disease than CM from Mauritius (low levels of genetic diversity) (Sharpe et al., 2017). Following inoculation, NHPs are considered to be infected on the basis of the same criteria as used for human diagnosis. *In vivo* imaging is of particular interest, in addition to Mtb growth in gastric aspirates (GA) and/or bronchoalveolar lavage (BAL) samples, conversion in an immunological diagnostic test (TST, IGRA), the presence of clinical signs (cough, weight loss), and transcriptomic findings (Capuano 3rd et al., 2003; Lin et al., 2013b). The exposure of CM to low doses of Mtb through aerosols leads to a form of latent TB resembling that in humans (Capuano 3rd et al., 2003). Latent TB in NHPs is defined by an absence of clinical signs, with no cultivable bacteria in BALs or gastric aspirates for at least six months, with evidence of infection (see above). Interestingly, like humans, CM can develop stable latent TB, spontaneously reactivated disease, or a reactivation of infectious disease in response to immune suppression (Lin et al., 2009). Studies in macaque models have shown that individual lesions may respond different to different drugs. Macaques and marmosets are also used in many vaccine studies, including studies of new routes of inoculation and new vaccine candidates.

The immune response to Mtb seen in macaques and humans following aerosol exposure is relatively slow. The cellular immune response leading to the formation of granulomas predominates. In humans and macaques, peripheral responses to Mtb infection can usually be detected after four to six weeks. The available data support the hypothesis that the outcome of Mtb infection is determined at granuloma level (Flynn et al., 2015). The use of *in vivo* imaging in NHPs revealed individual granulomas that were visible as early as two to four weeks after inoculation. These granulomas were dynamic, changing over time, and appeared to be independent of each other (Coleman et al., 2014; Lin et al., 2013a, 2014). Macaques often present classic lesions with central caseous and necrotic cores, but other types of granulomas (non-necrotizing, suppurative) have also been observed, as in humans (Scanga and Flynn, 2014). The key cells involved in granuloma formation are macrophages, dendritic cells and neutrophils, which promote Mtb antigen-specific Th1 responses, with the local secretion of large amounts of IFN-γ. Moreover, newly characterized components of the innate immune system, such as invariant natural killer T (iNKT) cells (Chancellor et al., 2017), MAIT cells (Bucsan et al., 2019; Paquin-Proulx et al., 2018) γδ T cells (Chen et al., 2013; Dan Huang et al., 2012; Janis et al., 1989), and ILC (Ardain et al., 2019), or the microbiota (Gupta et al., 2018) may play an important role in influencing the outcome of Mtb infection. Latent TB infection in NHPs has been activated by TNFα pathway blockade or by co-infection with TB in macaques infected with simian immunodeficiency virus (SIV), as a model of HIV infection in humans (Bucşan et al., 2019; Diedrich et al., 2010). Interestingly, studies in these models have raised the possibility of a CD4^{+} T cell–independent mechanism of latent TB control involving CD8^{+} T cells (Foreman et al., 2016).

As for RSV, the species is key in studies of Mtb: macaques and marmosets are the best species for studies aiming to improve our understanding of Mtb infection and to evaluate treatment and vaccination strategies against this pathogen. The studies discussed here also highlight the need for innovative tools for following the disease, with parameters comparable with those used in humans. This is also the case for other bacteria, such as *Bordetella pertussis*.

4.5. Whooping cough

Whooping cough, or pertussis, is a highly contagious respiratory disease caused by airway infection with *Bordetella pertussis*. In human patients, this disease is characterized by a prolonged characteristic cough lasting several weeks, an increase in circulating lymphocyte levels, and a transient fever. Over the last two decades, despite high levels of vaccination coverage (86 % on average; (WHO, 2018b), the number of whooping cough cases has been increasing in many countries (Centers for Disease and Prevention, 2019). Unfortunately, the causes of this resurgence remain poorly understood.

Bordetella pertussis infection models are, thus, crucial to improve our understanding of the pathophysiology of pertussis and the immune responses correlated with protection. Several non-primate preclinical models, including rodents and pigs, have been used in studies of whooping cough, but none of these models fully reproduces the spectrum of clinical symptoms, notably cough (Elahi et al., 2005; Elahi et al., 2007). Some studies have also been performed in NHPs. Cases of whooping cough in chimpanzees with classic clinical symptoms and controlled infection were reported decades ago (Rich et al., 1932). Many studies have also reported controlled *B. pertussis* infection tests in other NHP species, including RM and CM or cebus monkeys (Culotta et al., 1935; Merkel and Halperin, 2014). However, most of these studies reported a failure to provide a robust infection model reproducing all the clinical symptoms observed in humans, and cough in particular.

Baboons are currently the only available NHP model accurately reproducing most of clinical characteristics of pertussis in humans. *Papio anubis* monkeys exposed to *B. pertussis via* the IN and IT routes have been reported to develop a typical long-lasting paroxysmal cough, leukocytosis, mild fever and colonization of the upper airways (Naninck et al., 2018; Warfel et al., 2012a). Natural transmission between baboons has also been reported in the same basic model (Warfel et al., 2012c).

The immune responses occurring in baboons after *B. pertussis* exposure were then investigated, revealing the importance of the cellular Th1/Th17 T-cell response, in addition to the humoral response, for strong immunity and efficient bacterial clearance (Warfel et al., 2012a, b, Warfel et al., 2014b).

The first vaccination studies in baboons revealed that acellular pertussis vaccines were unable to prevent bacterial colonization and transmission (Warfel et al., 2014b). The findings for this preclinical model provided additional support for the hypothesis that current acellular vaccination protocols may have resulted in a pool of asymptomatic patients infected with *B. pertussis*, likely to contribute to the resurgence of whooping cough.

The baboon model of pertussis is now used in many vaccination studies, including studies of candidate vaccines, and may therefore contribute to the deciphering of immune correlates of protection and new vaccination strategies to protect against pertussis (Kapil et al., 2018; Locht et al., 2017; Warfel et al., 2014a, 2016).

This bacterium is, thus, even more restrictive than those discussed above in terms of the susceptibility of NHP species. Only baboons can be used to reproduce the features of the human disease accurately. A few other bacterial respiratory diseases have been studied in NHPs, but in much less detail.

4.6. Other bacteria

4.6.1. Streptococcus pneumoniae

S. pneumoniae causes pneumonia and is responsible for deaths worldwide. This bacterium is usually present in the human nasopharynx, and this colonization precedes infection of the lungs. In some individuals, it can also induce bacteremia and meningitis (McCullers and Tuomanen, 2001). *S. pneumoniae* pneumonia generally occurs as a secondary infection following infection with viruses, such as influenza or adenovirus. The typical clinical symptoms of pneumococcal pneumonia are chills, cough, hyperventilation, tachycardia, fever and a loss of appetite. Diagnosis is based on the presence of alveolar infiltration on chest X-rays and an increase in white blood cell counts. These parameters usually return to normal within three weeks.

Philipp et al. (Philipp et al., 2006) established a model of *S. pneumoniae* pneumonia in RM by IT inoculation, for use in vaccine assessment. RM are probably not natural carriers of *S. pneumoniae* (Philipp et al., 2012), but this study revealed that they were nevertheless

receptive to infection. Bacteria were detectable in BAL fluids three to five weeks post-inoculation, and infected macaques presented clinical signs of pulmonary infection (Philipp et al., 2006). None of the animals developed systemic infection. A loss of appetite and respiratory distress was observed in some of the animals, together with fever, but cough and tachycardia were not apparent. All animals displayed an increase in leukocyte counts and alveolar infiltration on chest X-rays. As in infected humans, IL-6, IL-1β and TNF-α levels in BAL were high at the onset of infection, and then rapidly returned to basal levels, except for IL-6, which remained present at high levels throughout the duration of the study. Similarly, neutrophil counts were high in the BAL of all infected animals. Thus, inoculation of the lungs of RM with *S. pneumoniae* reproduces most of the symptoms observed in infected humans.

This model has been used to test a vaccine, which was found to protect against pneumonia (Denoel et al., 2011).

A similar pneumonia model was established in baboons (*Papio cynocephalus*), which displayed similar symptoms, with the exception of bacteremia, which was present in all the infected animals 24 h post-infection (Reyes et al., 2017). This model was used to evaluate the cardiac toxicity of *S. pneumoniae* after pneumococcal pneumonia. In this study focusing on heart parameters, cardiac injury was observed in all infected animals, with ischemic alterations visible on electro- and echocardiography, and high serum troponin concentrations. On necropsy, *S. pneumoniae* was detected in the myocardium; necroptosis and apoptosis were observed in the heart tissue, together with scars, consistent with an acute cardiac toxicity syndrome. This model reproduces previous observations that one third of patients with *S. pneumoniae* lung infection experience major adverse cardiac events.

Superinfection models have also been created in NHPs, as most cases of *S. pneumoniae* respiratory disease result from underlying viral infection. In this context, CM were co-infected with an avian influenza virus (subtype H7N7) and *S. pneumoniae* (Miyake et al., 2010). However, inoculation with both these pathogens did not induce the severe pneumonia observed in co-infected human lungs, probably because the two pathogens were introduced simultaneously, whereas, in human patients, the viral infection precedes bacterial colonization. This model was nevertheless used to investigate the effect of a vaccine against H7N7 virus on co-infection-related morbidity (Miyake et al., 2010). Vaccination decreased the severity of pneumonia, demonstrating that anti-viral vaccination can also decrease the severity of bacterial infection in this context.

A co-infection model also shed light on the immunodepressive effect of acute ethanol intoxication in simian immunodeficiency virus (SIV)-infected RMs subsequently infected with *S. pneumoniae* (Nelson et al., 2013; Trevejo-Nunez et al., 2015).

4.6.2. Yersinia pestis

Plague, which is caused by *Yersinia pestis*, was historically a terrifying deadly disease, but can now be controlled by antibiotics. In addition to causing bubonic plague, *Y. pestis* can also cause lethal pneumonia in humans (Perry and Fetherston, 1997). On autopsy, the lung displays necrotizing pneumonia, with intra-alveolar edema and foci of severe alveolitis. After an initial lag period of 24−48 h, disease progression is rapid, with fever, tachypnea, tachycardia, bacteremia and blood leukocytosis.

RM and CM have been used as models for studies of pneumonic plague (Finegold, 1969; Koster et al., 2010; Van Andel et al., 2008), as have AGM (*Cercopithecus aethiops*) (Davis et al., 1996; Layton et al., 2011), which were infected with aerosolized *Y. pestis*. The inhalation of the bacterium rapidly leads to fatal disease, resembling that in humans. The histopathological features and clinical aspects of human plague are also observed during the course of infection in macaques. As in humans, infection required only a low bacterial load in monkeys. The disease also developed in two phases in primates. The features of human plague not observed in macaques are coughing, hemoptysis, thrombocytopenia and coagulopathy. These models have been used to study the effects of

vaccines and treatments (Cornelius et al., 2008; Honko et al., 2006; Huang et al., 2009).

4.6.3. Streptococcus pyogenes

S. pyogenes (also known as group A *Streptococcus*, GAS) is best known as a cause of pharyngitis, scarlet fever and impetigo (Carapetis et al., 2005). However, it can also trigger a severe form of bronchopneumonia, with notable outbreaks and a fatality rate of 30–60%. Histologically, the acute pneumonitis and bronchitis induced by *S. pyogenes* are characterized by a dense polymorphonuclear (PMN) leukocyte infiltrate and edema. Interstitial pneumonitis, perivasculitis, vasculitis and bronchiolitis are also prominent features.

The model of LRTI due to *S. pyogenes* established in CM (Olsen et al., 2010a) mimics the histopathology of infection in humans. The animals present transient bacteremia, and bacteria are also recovered from the spleen and kidneys on necropsy. The hilar lymph nodes display massive follicular expansion and sinus histiocytosis, characteristic of an exuberant immune response. The bone marrow is hyperplastic, due to expansion of the myeloid lineage and megakaryocytes. Serum concentrations of acute-phase proteins, such as CRP and fibrinogen, increase significantly. Serum concentrations of pro-inflammatory cytokines and peripheral WBC counts are high at 24 h, but decrease to baseline levels by 120 h, indicating that infection induces a robust inflammatory response that then rapidly decreases. The histological and clinical features observed in infected macaques are identical to those observed in humans with *S. pyogenes* pneumonia. However, the late phases of infection were not investigated in this study, as all the animals were euthanized on day 5.

4.6.4. Staphylococcus aureus

S. aureus is a major cause of serious infections worldwide, and is responsible for various types of infectious diseases, ranging from mild skin lesions to fatal invasive diseases. Cases of fatal pneumonia have been reported, especially when *S. aureus* secretes the Panton-Valentine leukocidin (PVL), a two-component pore-forming toxin targeting PMNs. PVL expression in bacteria is epidemiologically correlated with methicillin-resistant *S. aureus* (MRSA), which emerged in the 1990s and has a particularly high incidence in North America (Moran, 2006). This pathogen can cause fatal pneumonia.

An MRSA infection model has been established in CM, mimicking the clinical and histological features of mild-to-moderate *S. aureus* pneumonia in humans (Olsen et al., 2010b). However, the specific, and very severe effects of PVL were not observed. Furthermore, the use of a PVL-deficient strain yielded similar symptoms, confirming the lack of effect of PVL in NHPs. Community-acquired *S. aureus* pneumonia is often associated with viral infections. A co-infection model was therefore established by the same group in CM (Kobayashi et al., 2013). Animals were first infected with the H3N2 influenza virus, and then with MRSA five days later. However, viral infection failed to enhance *S. aureus* pathogenesis in the lungs. Another co-infection model was recently established in RMs, using influenza A virus instead of H3N2 and a bacterial inoculum three orders of magnitude larger (Chertow et al., 2016). The animals were first infected with influenza A, either by IB inoculation or by aerosolization, and then with MRSA by IB inoculation on day 4. Severe pneumonia was observed in the IB influenza alone and IB influenza plus MRSA groups. However, chest X-rays revealed larger amounts of infiltrate and more severe lung histopathology for the co-infection. This is the NHP model most closely resembling human *S. aureus* pneumonia, although PVL is probably not active because of species specificity.

4.6.5. Klebsiella pneumoniae

K. pneumoniae is an opportunistic pathogen that can cause various infectious diseases, including pneumonia, usually in individuals with comorbid conditions or susceptibility factors. A high proportion of strains are resistant to multiple antibiotics, accounting for the high

mortality associated with infections with this bacterium (Munoz-Price et al., 2013).

NHPs are naturally susceptible to *K. pneumoniae* infections, notably pneumonia. A model of *K. pneumoniae* lung infection in CM was recently established by IT inoculation (Malachowa et al., 2019). Severe pneumonia was observed on X-ray and pathology analyses, revealing edema, bronchiolitis, vasculitis and pleuritis. The infection resolved from day 11 onwards. This model was used to test a vaccine, which protected animals against severe disease (Malachowa et al., 2019).

All these bacteria have been studied in less depth than Mtb or *Bordetella pertussis*, mainly because they cause fewer hospitalizations or deaths and are easier to control with antibiotics. However, the risk of antibiotic-resistant bacteria emerging is growing, and such studies will therefore be of increasing importance in the coming years. They also highlight the importance of NHPs as models for studying co-infection with SIV or the effects of smoking on respiratory infectious diseases.

4.7. Conclusions

Many NHP species can be used as models for the study of respiratory pathogens, both viruses and bacteria. However, some species display symptoms more closely resembling those of humans than others, and these species should be used preferentially when assessing treatment or vaccine efficacy. But even if human symptoms are not fully reproduced, NHPs remain the closest model we have to humans. The efficacy of drugs or vaccines can be studied in these models, on the basis of viral or bacterial load. Immune responses may also be an adequate readout for vaccine immunogenicity. NHPs are also great models for studying co-infections or the effect of comorbid conditions on respiratory infectious diseases.

New technologies from clinical set-ups have been adapted for NHPs, to consolidate these models in terms of pathophysiology and clinical follow-up, and have much increased the value of these preclinical models.

5. New technologies for the modeling and exploration of respiratory tract infections

The data obtained to date for NHPs exposed to various respiratory pathogens confirm the relevance of NHPs as preclinical models for the evaluation of drugs and vaccines, and for studies of the clinical outcome of respiratory infectious diseases. However, over the years, it has become clear that the closer we get to a naturally occurring infection, the better the match between the symptoms observed and those of humans. It is therefore crucial to improve the process of exposure to the pathogen, to mimic the natural infection process as closely as possible. It is also important to be able to compare the clinical data obtained in hospitals to those obtained in preclinical studies. Fortunately, it is now possible to use clinical material that has been adapted for NHPs, such as nebulizers or *in vivo* imaging techniques.

5.1. Experimental exposure to pathogens and treatments

In humans, the RT is infected directly by contact between the hand and the nose and mouth, droplets produced by coughing, for example, or aerosols from various endogenous and exogenous sources. The direct deposition of respiratory pathogens, *via* the IN and/or IT routes, is probably the most widely used approach in the development of NHP models. Flexible endoscopy makes it possible to target a specific lung lobe more precisely, as in Mtb deposition (Sibley et al., 2016). However, these approaches do not mimic the natural transmission of airborne pathogens. Bioaerosol production, leading to pathogen transmission, takes place when we breathe, talk, laugh, cough and sneeze (Thomas, 2013). Systems for exposure to experimental aerosols have been under development for decades, to reproduce a natural exposure of the airways to pathogens (Alsved et al., 2020; Warfel et al., 2012b). Aerosol delivery

systems can be split into two parts: the aerosol generator and the exposure system or interface. Aerosol delivery systems provide an even distribution of the pathogenic agent throughout the pulmonary lobes, particularly in the cranial lobes, which are the easiest to target. Diverse aerosol-generating systems have been described, with specific characteristics in terms of particle concentration and size, and, thus, the distribution of deposits in the RT. The use of aerosol technology to expose the RT to the pathogen is crucial in models of respiratory infections and can influence disease severity by modifying the distribution of the pathogen on its anatomical or cellular target (Thomas, 2013). Indeed, pathogenesis in animal models of infectious diseases, such as influenza, may differ with the distribution of the virus in the lung (Watanabe et al., 2018). The circulation of aerosol particles in the airway, as a function of particle size and respiration physiology, is well described in humans, but not, as yet, in all NHP models (Kulkarni et al., 2016). Basically, in adults, particles of more than 5 μm in diameter remain in the URT, particles between 2 and 5 μm in diameter are deposited in the lower airways and particles between 0.5 and 2 μm in diameter are deposited in the alveoli (ISO, 2013; Standardization, 2007). Submicronic particles (smaller than 0.5 μm in diameter) are mostly exhaled or diffuse into the bloodstream *via* the vascular system of the lung. These theoretical distributions for humans may not apply to NHPs. They have been explored *in vivo* in macaques, with innovative imaging tools, such as PET imaging. These studies highlighted the possibility of using clinical aerosol generators in macaques in a translational research approach (Dabisch et al., 2017).

In addition to particle size, which determines the anatomical site of deposition of the aerosol, other factors must be taken into account when exposing NHPs to pathogen-containing aerosols. The constraints imposed by the use of NHP models and highly infectious pathogens limit the possibility of exposing awake animals to the pathogen. Exposure under anesthesia is preferred, but this influences respiratory rate, breathing magnitude and airflow in the URT. The interface between the aerosol generator and the animal is also a key point, and various approaches have been described: isolator, face mask or IT intubation (Wong, 2007), as described in Table 1.

Nebulizers are liquid atomizer systems widely used for aerosol generation in clinical practice and capable of producing a highly respirable fraction (particles less than 5 μm in diameter). Several types of nebulizers, producing aerosols with different characteristics, are available, as detailed in Table 2. Three major technologies have been used in NHP models. The jet nebulizer is the oldest technology used for pathogen exposure. The sizes of the particles produced depend on air/gas pressure. The ultrasonic nebulizer uses piezoelectric quartz vibration to generate aerosols of specific particle size as a function of wave frequency. Finally, mesh nebulizers form aerosols by passing pathogen suspensions through a perforated membrane, which determines particle size.

However, some inoculum properties may not be compatible with all three nebulization techniques. For instance, the inoculum must contain large particles or have a high viscosity for ultrasonic and mesh nebulizers. Conversely, heat-sensitive pathogens are unsuitable for ultrasonic nebulization and shear-sensitive pathogens cannot be used with jet nebulizers. Targeting a specific part of the tract can therefore be a real technological challenge.

The concentration and size of droplets must be accurately measured, to guarantee the homogeneity of NHP exposure, to determine the volumes of aerosol inhaled, and to ensure reproducibility. The coupling of the device to a plethysmograph makes it possible to calculate the amounts inhaled as a function of the ventilatory parameters of the animals (Alsved et al., 2020; Hartings and Roy, 2004; Wong, 2007). In addition, real-time capture tools (impinger), designed to impose minimum stress on the microorganism, can be used to determine pathogen concentrations and viability.

All three types of nebulizers are used in NHPs. They each have advantages and disadvantages (Table 2) that must be taken into account by users.

Table 1
Advantages and limitations of the various interfaces for NHP exposure to respiratory pathogens.

Interfaces	Advantages	Disadvantages
Intra-tracheal instillation	Easy	Lung distribution not uniform
	Allows to deposit a precise quantity	Anesthetized NHPs
	Repeatable	Apnea during the exposure
		By-pass URT defense mechanisms
Endo-tracheal nebulization	Homogeneous deposition	Anesthetized NHPs
	Relatively repeatable	Mechanical ventilation during the administration
		By-pass URT defense mechanisms
Head only chamber	Non-invasive	
	Anesthesia not mandatory	Face and eyes exposure
	Spontaneous breathing	Reduced air flow in the chamber
	Ideal for repeated dose studies	Aerosol volume loss
	Several animals possible at the same time	
Whole body cabinet	Non-invasive	Full body contamination (fur, skin, eyes),
	Vigilant animal	Reduced air flow in the chamber
	Spontaneous breathing	Heat accumulation
	Ideal for prolonged exposure studies	Bulky and expensive
	Several animals possible at the same time	Substantial aerosol volume loss
Oronasal face mask	Easy	
	Spontaneous breathing	Air leakage
	Reduced aerosol volume loss	Face and eyes exposure
	Mouth and nose targeting	Anesthetized animal
Nose piece	Easy	Air leakage
	Spontaneous breathing	High deposition in nasal cavities
	Reduced aerosol volume loss	Anesthetized animal

5.1.1. Jet nebulizers

Jet nebulization is the oldest technology available and is widely used in animal models of infection. It uses a gas source to atomize the liquid into fine particles. Around 90 % of large particles fall back in the nebulizer reservoir, resulting in a change of concentration and viability of the pathogen over time. Particles are polydispersed and their size depends on the airflow. These devices are suitable for producing low MMAD (mass median aerodynamic diameter) particles for targeting deep within the lungs (1–2 µm and down to submicronic particle sizes, 0.2 µm). One of their principal limitations is the difficulty changing aerosol flow without changing aerosol particle size, with the aerosols generated by a nozzle. The volume of air required to generate and transport the aerosols is often greater than the volume that the animals can breathe, resulting in a significant loss of inoculum in inhalation chambers. The flow rate is often too high (6–8 L/min used for a standard jet nebulizer *vs*. 1−2 L/min for NHPs) as the animals are anesthetized for face-mask delivery or mechanical ventilation (exposure *via* an IT tube).

One of the major advantages of these devices is the possibility of nebulizing suspensions and viscous solutions. Je nebulizers are, therefore, the preferred technology for the nebulization of bacteria. Inoculum volume is often at least 10 mL (three-jet collision) and it is difficult to nebulize small volumes due to the residual volume. Calculation of the amounts of inhaled particles is straightforward because the aerosol is reproducible.

5.1.2. Ultrasonic nebulizers

In ultrasonic nebulizers, the size of the particles generated is a function of the frequency of the ultrasonic waves. Particle size is fixed during a procedure (polydispersal of the aerosol). The degradation of heat-sensitive molecules due to quartz warming is the principal drawback of these nebulizers. They are not suitable for the generation of suspensions. Like jet nebulizers, some residual mass is trapped in the nebulizer, and liquid concentration increases over time. By contrast to jet nebulizers, the air flow rate can be adjusted to the minute ventilation of the animal without affecting aerosol generation (*i.e.* particle size). Users may also encounter difficulties washing and decontaminating the equipment, making it unsuitable for the generation of bioaerosols.

5.1.3. Mesh nebulizers

These devices have membranes that contain holes of a perfectly characterized size (2−4 µm). The size of the droplets generated is fixed, unless the holes become blocked with aggregates. As with the ultrasonic nebulizer, airflow can be modified without changing the size of the droplets. Mesh nebulizers are, therefore, perfectly suitable for use in anesthetized animals, whether breathing spontaneously or on mechanical ventilation (after intubation or with a facemask). One of the limitations of this technology is the requirement for the inoculum to be free of particles larger than the holes in the mesh. It is also impossible to nebulize liquids that are too viscous.

Mesh nebulization thus appears to be less aggressive to the inoculum than jet or ultrasonic nebulization, due to the physical mechanism of droplet generation and the absence of droplet recycling in the reservoir. This results in a constant formulation in the reservoir, and, thus, the maintenance of constant amounts of aerosol over time. It is highly suitable for the exposure of animals to viruses, as it limits losses of viability (Bowling et al., 2019) with a fairly small volume (less than 1 mL).

Aerosols are also effective for the delivery of vaccines or treatment to the RT (Castro et al., 2005; Mathieu et al., 2013). Combining the advantages of low residual volume with adjustable airflow, mesh nebulizers provide highly efficient deposition in terms of the volume loaded in the reservoir.

As described above, the nasal anatomy of primates, and of RM in particular, is similar to that of humans. This features of NHPs makes it possible to use the same IN deposition techniques in translational approaches, in preclinical studies in NHPs and in humans (Yeh et al., 1997). Macaques are highly suitable models for neonatal aerosol deposition (Dubus et al., 2005). NHPs seem to have a high degree of exposure to inhaled substances, particularly in terms of deposition per unit of airway surface area. However, the different alveolar volumes in the RM model had only minor effects on aerosol dosimetry within the lungs by imaging techniques (scintigraphy with [99Tc] or other techniques; (Cheng et al., 2008). The breathable particle size for RM (Dabisch et al., 2017; Wolff, 1996) should be considered different from that for adult humans, and closer to that for human children (*i.e.* 2.4 µm *vs* 5 µm)(Schuepp et al., 2009; Schuepp et al., 2005).

Depending on the pathogen, NHP species and aim of the study, it is now possible to choose between various exposure techniques to improve both the relevance and reproducibility of preclinical studies. Once the best model in terms of pathophysiology has been selected, it is also important to choose the best way to follow the disease *in vivo* and to ensure comparability to clinical data.

5.2. In vivo imaging to monitor the infection

Many approaches are used to monitor respiratory infections, including blood sampling, swabs, curettage or more extensive lavages of the RT. However, most of these approaches are quite invasive provide only very local information, or, conversely, a global but poorly resolved picture of the whole infection. *In vivo* imaging at local and/or at whole-body scale is a better way of exploring respiratory infections longitudinally without invasive sampling.

Various imaging strategies can be considered. Chest X-rays are a useful, easily implemented technique. Their limitless depth of

Table 2

Different types of aerosol nebulizers used in NHP models.

Nebulizer technology	Nebulization specification	Animal exposure interface	Aerosols characteristics		Key Facts	Field of expertise	NPH species	Refs.
			Type	MMAD				
Jet Nebulizer	3 Jet-Collision	Head only Exposure inhalation chamber	Rift Valley Fever Encephalitis (RVFV); strain ZH501.	Not specified	Development of neurological disease in AGM	Virology Physiopathology Treatment.	AGM	(Wonderlich et al., 2017)
		Head only Exposure inhalation chamber	Nipah Virus (NV)	11,0–12,5 μm	Large particles of NV target extra thoracic regions and nasopharynx	Virology Physiopathology	AGM	(Lee et al., 2020)
				0,5–3 μm	Small particles of NV reach the deep lungs and induce diffuse pulmonary disease			(Cong et al., 2017)
				6,5–8μm	Intermediate particles of NV induce pulmonary parenchymal disease and brain lesions			(Hammoud et al., 2018)
		Head only Exposure inhalation chamber	Monkeypox Virus	1,2μm	Monkeypox virus in macaques	Virology Physiopathology	CM	(Zaucha et al., 2001)
		Exposure Box, Cabinet	Anthrax: Aqueous suspension of virulent strain of Bacillus anthracis spores	1–2μm	Gross and microscopic anatomopathological lesions	Bacteriology, Biodefense, Countermeasures	CM	(Vasconcelos et al., 2003)
	3 Jet Nebulizers (Nanoneb®, Atomisor Nl11, Sidestream) Q = 8 L/min		Polydispersed Aerosols of DTPA -Tc99m	0.15 μm–0.5 μm 0.25 μm–1 μm, Sidestream 1 μm–9 μm, Nanoneb	Regional deposition patterns Deposition in thoracic region *vs* extra thoracic region	Clinical development	Baboons *Papio anubis*	(Albuquerque-Silva et al., 2014)
Ultrasonic Nebulizer	Ultrasonic	Oronasal Mask	Radiolabed Monodispersed aerosols	1.7, 3.6, 7.4 and 11.8 μm	Regional deposition pattern shifts as particles size increases, greater deposition in proximal regions of the respiratory tract	Toxicology / deposition pattern	RM	(Dabisch et al., 2017)
Mesh Nebulizer	Aeroneb®, Vibrating Mesh Nebulizer	Exposure inhalation chamber (total airflow of 16 L/min)	SARS-CoV-2 Virus size: 60 and 140 nm Polydisperse small particles aerosol *vs* multi-route mucosal exposure	1,7μm	Pulmonary inflammation and lymph nodes invasion. Pneumonia visible by *in vivo* imaging ([^{18}F]-FDG/PET/CT)	Virology and vaccinology	AGM	(Hartman et al., 2020)

penetration can provide an overview of an entire lung in a single image. Density abnormalities detected on X-rays can reveal and characterize pneumonia and infection patterns. This technique remains the most widely used type of imaging for the monitoring of infection, including the recent monitoring of SARS-CoV-2 infection in NHPs (Deng et al., 2020b; Williamson et al., 2020). However, X-rays provide analyses of the RT in only two dimensions and their spatial resolution is relative poor (of the order of a few millimeters). Computed tomography (CT-scans) can provide a three-dimensional tomographic reconstruction of the lungs at much higher resolution (500 μm to 1 mm). It can also be used for quantitative analyses of density (expressed in Hounsfield units). The percentage change in lung hyperdensity (PCLH) has recently been proposed as a means of monitoring COVID-19 lung burden in a quantitative manner in SARS-CoV-2-infected NHPs (Finch et al., 2020), with more conventional, but operator-dependent, semi-quantitative CT scoring based on lesion type and extension.

Functional *in vivo* imaging can also be used to monitor respiratory infections in NHPs. Positron emission tomography (PET) coupled to CT is a key tool for monitoring in NHPs and could be used for prognostic purposes, for the prediction of successful drug treatment for TB (Lin et al., 2013a). [^{18}F]-Fluorodeoxyglucose, a glucose analog trapped in cells, is the most common tracer used in PET imaging. This radiotracer is a quantitative marker of cell hypermetabolism, as depicted in Fig. 1, and it therefore reflects inflammation, such as granuloma activity or the presence of inflammatory cell infiltrates, for instance.

Other radiotracers for direct pathogen visualization, such as fluorodeoxysorbitol and fluoromaltose (Gowrishankar et al., 2014; Weinstein et al., 2014), sugars specifically metabolized by some enterobacteria, with a broad rapid biodistribution, as a means of increasing specificity. Radiolabeled antibodies targeting pulmonary pathogens are also currently undergoing validation in small-animal models (Rolle et al., 2016; Thornton, 2018; Wiehr et al., 2016), and may be rapidly transposed to NHP studies, as already reported for SIV monitoring in macaques (Santangelo et al., 2015). Several limitations, such as liver uptake and slow biodistribution due to the biological nature of antibodies may also be taken into account, but can be overcome by modifying the probe. Antibody radiotracers and their derivatives (diabodies, minibodies, nanobodies, *etc.*) are promising tools for the specific detection of respiratory pathogens, despite potential issues relating to biodistribution and background (Freise and Wu, 2015).

One of the main advantages of the nuclear imaging techniques described above is that they are routinely used in clinical practice, facilitating the transfer of methods and results from preclinical studies into clinical practice. In addition, PET technology can be used for standardized quantitative signal assessment (expressed as the standard uptake value, SUV) with excellent sensitivity in defined regions of interest (Slomka et al., 2016). However, PET imaging cannot be used for multiplexing and sometimes also requires extensive radiochemistry and large installations with a high level of biosafety, which can limit its use.

Other optical imaging techniques, such as pulmonary bronchoscopy coupled with probe-based endomicroscopy, have also been used in NHPs and in other preclinical respiratory infection studies, with genetically modified fluorescent pathogens or probes. This last approach makes it possible to follow the distribution of the pathogen in the lower airways with excellent sensitivity and spatial resolution, but is still rarely used in infectious disease research (Thiberville et al., 2007, 2009) (Naninck et al., 2018). Optical imaging-based methods (fluorescence microscopy, two-photon microscopy, bioluminescence) suffer the disadvantage of a rapid loss of signal with the body of the NHP *in vivo* in the absence of heavy surgical intervention. However, these techniques can be used in smaller animal models, such as mice (Fiole et al., 2014; Fiole and Tournier, 2016).

In vivo imaging is highly advantageous for monitoring, with minimal invasiveness, the anatomical and functional respiratory burden following infection in NHPs, thanks to classical X-ray imaging and recent improvements in nuclear PET imaging. These techniques combine the advantages of closeness to clinical practice and of overcoming certain ethical issues in preclinical studies.

6. Ethical constraints and considerations for NHP studies

Throughout this review, one key issue arises concerning the use of NHPs as models for research purposes: ethics. Societal pressure has led to the emergence of laws regulating the use of animals, particularly NHPs, in biomedical research. Ethical guidelines such as the 4Rs (Reduce, Refine, Replace, Rehabilitate) must be taken into account, imposing various constraints, for projects to gain approval from ethics committees. A synergy between the need for solid answers to scientific questions and the consideration of animal welfare has made it possible to optimize the work with NHPs.
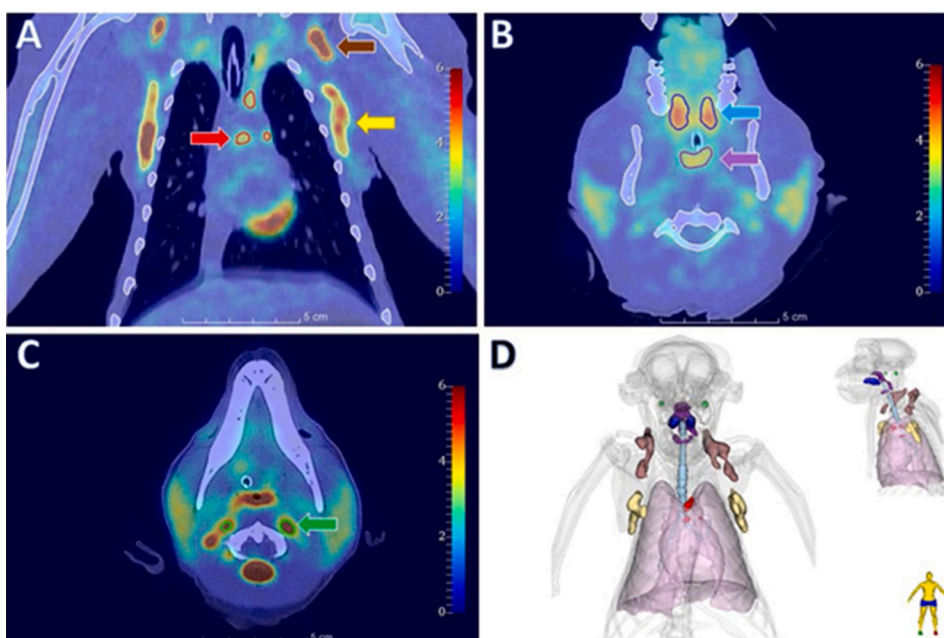

Fig. 1. PET-CT images of [^{18}F]-FDG uptake in a cynomolgus macaque.
(A) Chest frontal slice with lymph node hypermetabolism in the clavicular (brown arrow), mediastinal (red arrow) and axillary (yellow arrow) regions. **(B-C)** Transverse slice with hypermetabolism in the tonsil (blue arrow), nasopharynx-associated lymphoid tissue (purple arrow) and lymph node in cervical regions (green arrow). **(D)** 3D representation of [^{18}F]-FDG hypermetabolism.

Reducing the number of NHPs used per study is probably the most important goal worldwide for both ethical and practical reasons. The need for NHPs as preclinical models has increased in recent decades and will probably remain high with the emergence of new pathogens.

Firstly, these models must be restricted to research that are impossible with other animal models and to advanced phases of preclinical research. Statistical modelling now makes it possible to reduce the number of animals per group, by helping both the design and the analysis of the study.

Secondly, the use of wild-caught primates is banned since 1975 by the Convention on International Trade in Endangered Species of Wild Fauna and Flora (CITES) and all primates used in research in the European Union (EU) originate from approved breeding centers (CITES, 1973). In addition, the use of great apes as research models has progressively decreased and is now forbidden, which has necessitated the development of other NHP models over the years.

The need for breeding facilities with self-sustaining colonies has therefore increased. Up till now, laboratories have been allowed to work with F1 animals (*i.e.* born in a breeding facility, but born to wild-caught parents). However, this rule is due to change shortly in the European Union, with only the study of F2 generations permitted in laboratories, as a strict application of the 2010/63/UE directive. This regulatory change implies years of breeding to ensure that F2 animals are produced in similar numbers to the F1 animals currently used (PMS Limited, 2017). As it has been announced in 2017, breeding facilities will hopefully have had the time to adapt themselves.

In order to refine the protocols, and for NHPs to behave in a natural manner, they need to be kept in social groups, which can be complicated in infectious disease studies, in which transmission is an issue. The space required for each animal is much larger than that for small-animal models, making it necessary to have large and expensive dedicated rooms. Environmental enrichments to compensate for the constraints imposed on the animals and to reproduce their cognitive or feeding behaviors are constantly improved (NC3Rs, 2017). Cooperative work (target training, for example) is often used to reduce the experimental bias associated with repeated anesthesia (DeMarco and Nunamaker, 2019). The impact of stress on the pathophysiology of infectious diseases has been widely documented (Irwin and Cole, 2011; Padro and Sanders, 2014; Sloan et al., 2007), and the refinement of experimental procedures is necessary to obtain robust scientific data that can be directly transposed to humans.

It is also generally difficult to rehabilitate NHPs, due to the cost of accommodating such species over time, particularly after their use in infectious disease studies.

On another very positive note, the 4R rule has stimulated the search for new technologies. As we have discussed in this review, nebulization and *in vivo* imaging techniques are prime examples of technologies at our disposition for refining protocols thanks to minimally invasive techniques. In general, clinical techniques are easy to transpose to NHPs. *In vivo* imaging also makes it possible to decrease the number of animals required as the pathophysiology of a disease can be followed without needing to kill the animal.

7. Conclusions and perspectives

NHP models are precious tools for all stages of preclinical studies, providing us with a better understanding of infections and making it possible to test vaccines and drugs with parameters as close as possible to those in humans. Despite the costs, and the ethical and technical issues associated with NHP studies, recent years have seen the adaptation of many tools to NHPs, which can now be monitored with materials remarkably similar to that used in human medicine. Many human reagents are directly functional in NHPs, resulting in more straightforward comparisons than for small animals. Even if they do not perfectly reproduce the symptoms observed in humans for all pathogens, these precious models are of the utmost importance in the context of emerging pathogens and pandemics, as they can make it possible to predict the potential effects of a drug or vaccine in humans more accurately than small animal models, and more rapidly than clinical trials.

References

Albuquerque-Silva, I., Vecellio, L., Durand, M., Avet, J., Le Pennec, D., de Monte, M., Montharu, J., Diot, P., Cottier, M., Dubois, F., Pourchez, J., 2014. Particle deposition in a child respiratory tract model: in vivo regional deposition of fine and ultrafine aerosols in baboons. PLoS One 9, e95456.

Alsved, M., Bourouiba, L., Duchaine, C., Löndahl, J., Marr, L.C., Parker, S.T., Prussin, A. J., Thomas, R.J., 2020. Natural sources and experimental generation of bioaerosols: challenges and perspectives. Aerosol Sci. Technol. 54, 547–571.

Altamirano-Lagos, M.J., Diaz, F.E., Mansilla, M.A., Rivera-Perez, D., Soto, D., McGill, J. L., Vasquez, A.E., Kalergis, A.M., 2019. Current animal models for understanding the pathology caused by the respiratory syncytial virus. Front. Microbiol. 10, 873.

Andabaka, T., Nickerson, J.W., Rojas-Reyes, M.X., Rueda, J.D., Bacic Vrca, V., Barsic, B., 2013. Monoclonal antibody for reducing the risk of respiratory syncytial virus infection in children. Cochrane Database Syst. Rev., CD006602

Arabi, Y.M., Balkhy, H.H., Hayden, F.G., Bouchama, A., Luke, T., Baillie, J.K., Al-Omari, A., Hajeer, A.H., Senga, M., Denison, M.R., Nguyen-Van-Tam, J.S., Shindo, N., Bermingham, A., Chappell, J.D., Van Kerkhove, M.D., Fowler, R.A., 2017. Middle east respiratory syndrome. N. Engl. J. Med. 376, 584–594.

Ardain, A., Domingo-Gonzalez, R., Das, S., Kazer, S.W., Howard, N.C., Singh, A., Ahmed, M., Nhamoyebonde, S., Rangel-Moreno, J., Ogongo, P., Lu, L., Ramsuran, D., de la Luz Garcia-Hernandez, M., K Ulland, T., Darby, M., Park, E., Karim, F., Melocchi, L., Madansein, R., Dullabh, K.J., Dunlap, M., Marin-Agudelo, N., Ebihara, T., Ndung'u, T., Kaushal, D., Pym, A.S., Kolls, J.K., Steyn, A., Zúñiga, J., Horsnell, W., Yokoyama, W.M., Shalek, A.K., Kløverpris, H.N., Colonna, M., Leslie, A., Khader, S.A., 2019. Group 3 innate lymphoid cells mediate early protective immunity against tuberculosis. Nature 570, 528–532.

Arikata, M., Itoh, Y., Okamatsu, M., Maeda, T., Shiina, T., Tanaka, K., Suzuki, S., Nakayama, M., Sakoda, Y., Ishigaki, H., Takada, A., Ishida, H., Soda, K., Pham, V.L., Tsuchiya, H., Nakamura, S., Torii, R., Shimizu, T., Inoko, H., Ohkubo, I., Kida, H., Ogasawara, K., 2012. Memory immune responses against pandemic (H1N1) 2009 influenza virus induced by a whole particle vaccine in cynomolgus monkeys carrying Mafa-A1*052:02. PLoS One 7, e37220.

Babu, P.G., Selvan, A., Christuraj, S., David, J., John, T.J., Simoes, E.A., 1998. A primate model of respiratory syncytial virus infection. Indian J. Exp. Biol. 36, 758–762.

Bao, L., Deng, W., Huang, B., Gao, H., Liu, J., Ren, L., Wei, Q., Yu, P., Xu, Y., Qi, F., Qu, Y., Li, F., Lv, Q., Wang, W., Xue, J., Gong, S., Liu, M., Wang, G., Wang, S., Song, Z., Zhao, L., Liu, P., Zhao, L., Ye, F., Wang, H., Zhou, W., Zhu, N., Zhen, W., Yu, H., Zhang, X., Guo, L., Chen, L., Wang, C., Wang, Y., Wang, X., Xiao, Y., Sun, Q., Liu, H., Zhu, F., Ma, C., Yan, L., Yang, M., Han, J., Xu, W., Tan, W., Peng, X., Jin, Q., Wu, G., Qin, C., 2020. The pathogenicity of SARS-CoV-2 in hACE2 transgenic mice. Nature 583, 830–833.

Baskin, C.R., Bielefeldt-Ohmann, H., Garcia-Sastre, A., Tumpey, T.M., Van Hoeven, N., Carter, V.S., Thomas, M.J., Proll, S., Solorzano, A., Billharz, R., Fornek, J.L., Thomas, S., Chen, C.H., Clark, E.A., Murali-Krishna, K., Katze, M.G., 2007. Functional genomic and serological analysis of the protective immune response resulting from vaccination of macaques with an NS1-truncated influenza virus. J. Virol. 81, 11817–11827.

Bassett, L., Troncy, E., Robichaud, A., Schuessler, T.F., Pouliot, M., Ascah, A., Authier, S., 2014. Non-invasive measure of respiratory mechanics and conventional respiratory parameters in conscious large animals by high frequency Airwave Oscillometry. J. Pharmacol. Toxicol. Methods 70, 62–65.

Bates, J.T., Pickens, J.A., Schuster, J.E., Johnson, M., Tollefson, S.J., Williams, J.V., Davis, N.L., Johnston, R.E., Schultz-Darken, N., Slaughter, J.C., Smith-House, F., Crowe Jr, J.E., 2016. Immunogenicity and efficacy of alphavirus-derived replicon vaccines for respiratory syncytial virus and human metapneumovirus in nonhuman primates. Vaccine 34, 950–956.

Belshe, R.B., Richardson, L.S., London, W.T., Sly, D.L., Lorfeld, J.H., Camargo, E., Prevar, D.A., Chanock, R.M., 1977. Experimental respiratory syncytial virus infection of four species of primates. J. Med. Virol. 1, 157–162.

Bem, R.A., Domachowske, J.B., Rosenberg, H.F., 2011. Animal models of human respiratory syncytial virus disease. Am. J. Physiol. Lung Cell Mol. Physiol. 301, L148–156.

Berendt, R.F., 1974. Simian model for the evaluation of immunity to influenza. Infect. Immun. 9, 101–105.

Berkhoff, E.G.M., Geelhoed-Mieras, M.M., Fouchier, R.A.M., Osterhaus, A., Rimmelzwaan, G.F., 2007. Assessment of the extent of variation in influenza A virus cytotoxic T-lymphocyte epitopes by using virus-specific CD8+ T-cell clones. J. Gen. Virol. 88, 530–535.

Bluemel, J., 2015. The Nonhuman Primate in Nonclinical Drug Development and Safety Assessment. Elsevier/AP, Academic Press is an imprint of Elsevier, Amsterdam ; New York.

Boon, A.C., de Mutsert, G., Graus, Y.M., Fouchier, R.A., Sintnicolaas, K., Osterhaus, A.D., Rimmelzwaan, G.F., 2002. The magnitude and specificity of influenza A virus-specific cytotoxic T-lymphocyte responses in humans is related to HLA-A and -B phenotype. J. Virol. 76, 582–590.

Boukhvalova, M.S., Prince, G.A., Blanco, J.C., 2009. The cotton rat model of respiratory viral infections. Biologicals 37, 152–159.

Bouvier, N.M., Lowen, A.C., 2010. Animal models for influenza virus pathogenesis and transmission. Viruses 2, 1530–1563.

Bowling, O'Malley, Klimstra, Hartman, Reed, 2019. A Vibrating Mesh Nebulizer as an Alternative to the Collison Three-Jet Nebulizer for Infectious Disease Aerobiology. Appl. Environ. Microbiol. 85 (17) https://doi.org/10.1128/AEM.00747-19.

Brouwer, P.J.M., Brinkkemper, M., Maisonnasse, P., Dereuddre-Bosquet, N., Grobben, M., Claireaux, M., de Gast, M., Marlin, R., Chesnais, V., Diry, S., Allen, J.D., Watanabe, Y., Giezen, J.M., Kerster, G., Turner, H.L., van der Straten, K., van der Linden, C.A., Aldon, Y., Naninck, T., Bontjer, I., Burger, J.A., Poniman, M., Mykytyn, A.Z., Okba, N.M.A., Schermer, E.E., van Breemen, M.J., Ravichandran, R., Caniels, T.G., van Schooten, J., Kahlaoui, N., Contreras, V., Lemaitre, J., Chapon, C., Fang, R.H.T., Villaudy, J., Sliepen, K., van der Velden, Y.U., Haagmans, B.L., de Bree, G.J., Ginoux, E., Ward, A.B., Crispin, M., King, N.P., van der Werf, S., van Gils, M.J., Le Grand, R., Sanders, R.W., 2021. Two-component spike nanoparticle vaccine protects macaques from SARS-CoV-2 infection. Cell 184 (1188-1200), e1119.

Bucşan, A.N., Chatterjee, A., Singh, D.K., Foreman, T.W., Lee, T.-H., Threeton, B., Kirkpatrick, M.G., Ahmed, M., Golden, N., Alvarez, X., Hoxie, J.A., Mehra, S., Rengarajan, J., Khader, S.A., Kaushal, D., 2019. Mechanisms of reactivation of latent tuberculosis infection due to SIV coinfection. J. Clin. Invest. 129, 5254–5260.

Bucsan, A.N., Rout, N., Foreman, T.W., Khader, S.A., Rengarajan, J., Kaushal, D., 2019. Mucosal-activated invariant T cells do not exhibit significant lung recruitment and proliferation profiles in macaques in response to infection with Mycobacterium tuberculosis CDC1551. Tuberculosis Edinb. (Edinb) 116S, S11–S18.

Cadena, A.M., Klein, E.C., White, A.G., Tomko, J.A., Chedrick, C.L., Reed, D.S., Via, L.E., Lin, P.L., Flynn, J.L., 2016. Very low doses of Mycobacterium tuberculosis yield diverse host outcomes in common marmosets (Callithrix jacchus). Comp. Med. 66, 412–419.

Capuano 3rd, S.V., Croix, D.A., Pawar, S., Zinovik, A., Myers, A., Lin, P.L., Bissel, S., Fuhrman, C., Klein, E., Flynn, J.L., 2003. Experimental Mycobacterium tuberculosis infection of cynomolgus macaques closely resembles the various manifestations of human M. tuberculosis infection. Infect. Immun. 71, 5831–5844.

Carapetis, J.R., Steer, A.C., Mulholland, E.K., Weber, M., 2005. The global burden of group A streptococcal diseases. Lancet Infect. Dis. 5, 685–694.

Casadei, E., Salinas, I., 2019. Comparative models for human nasal infections and immunity. Dev. Comp. Immunol. 92, 212–222.

Castleman, W.L., Dungworth, D.L., Tyler, W.S., 1975. Intrapulmonary airway morphology in three species of monkeys: a correlated scanning and transmission electron microscopic study. Am. J. Anat. 142.

Castro, J.F., Bennett, J.V., Rincon, H.G., Munoz, M.T., Sanchez, L.A., Santos, J.I., 2005. Evaluation of immunogenicity and side effects of triple viral vaccine (MMR) in adults, given by two routes: subcutaneous and respiratory (aerosol). Vaccine 23, 1079–1084.

Centers for Disease, C., Prevention, 2019. Pertussis | Surveillance Trend Reporting and Case Definition. CDC.

Cesta, M.F., 2006. Normal structure, function, and histology of mucosa-associated lymphoid tissue. Toxicol. Pathol. 34, 599–608.

Chan, J.F.-W., Yao, Y., Yeung, M.-L., Deng, W., Bao, L., Jia, L., Li, F., Xiao, C., Gao, H., Yu, P., Cai, J.-P., Chu, H., Zhou, J., Chen, H., Qin, C., Yuen, K.-Y., 2015. Treatment with Lopinavir/Ritonavir or Interferon-β1b improves outcome of MERS-CoV infection in a nonhuman primate model of common marmoset. J. Infect. Dis. 212, 1904–1913.

Chan, J.F., Yuan, S., Zhang, A.J., Poon, V.K., Chan, C.C., Lee, A.C., Fan, Z., Li, C., Liang, R., Cao, J., Tang, K., Luo, C., Cheng, V.C., Cai, J.P., Chu, H., Chan, K.H., To, K. K., Sridhar, S., Yuen, K.Y., 2020. Surgical mask partition reduces the risk of noncontact transmission in a golden syrian Hamster model for coronavirus disease 2019 (COVID-19). Clin. Infect. Dis. 71, 2139–2149.

Chancellor, A., White, A., Tocheva, A.S., Fenn, J.R., Dennis, M., Tezera, L., Singhania, A., Elliott, T., Tebruegge, M., Elkington, P., Gadola, S., Sharpe, S., Mansour, S., 2017. Quantitative and qualitative iNKT repertoire associations with disease susceptibility and outcome in macaque tuberculosis infection. Tuberculosis Edinb. (Edinb) 105, 86–95.

Chandrashekar, A., Liu, J., Martino, A.J., McMahan, K., Mercad, N.B., Peter, L., Tostanosk, L.H., Yu, J., Maliga, Z., Nekorchuk, M., Busman-Sahay, K., Terry, M., Wriji, L.M., Ducat, S., Martine, D.R., Atyeo, C., Fischinger, S., Burk, J.S., Slei, M.D., Pessaint, L., Van Ry, A., Greenhouse, J., Taylor, T., Blade, K., Cook, A., Finneyfrock, B., Brown, R., Teow, E., Velasco, J., Zahn, R., Wegmann, F., Abbink, P., Bondzi, E.A., Dagotto, G., Gebr, M.S., He, X., Jacob-Dolan, C., Kordana, N., Li, Z., Lifto, M.A., Mahrokhia, S.H., Maxfiel, L.F., Nityanandam, R., Nkolol, J.P., Schmid, A. G., Mille, A.D., Bari, R.S., Alter, G., Sorge, P.K., Este, J.D., Andersen, H., Lewi, M.G., Barou, D.H., 2020. SARS-CoV-2 infection protects against rechallenge in rhesus macaques. Science 369, 812–817.

Chen, C.Y., Yao, S., Huang, D., Wei, H., Sicard, H., Zeng, G., Jomaa, H., Larsen, M.H., Jacobs, W.R., Wang, R., Letvin, N., Shen, Y., Qiu, L., Shen, L., Chen, Z.W., 2013. Phosphoantigen/IL2 Expansion and Differentiation of Vγ2Vδ2 T Cells Increase Resistance to Tuberculosis in Nonhuman Primates. PLoS Pathog. 9, e1003501.

Cheng, Y.S., Irshad, H., Kuehl, P., Holmes, T.D., Sherwood, R., Hobbs, C.H., 2008. Lung deposition of droplet aerosols in monkeys. Inhal. Toxicol. 20, 1029–1036.

Chertow, D.S., Kindrachuk, J., Sheng, Z.M., Pujanauski, L.M., Cooper, K., Nogee, D., Claire, M.S., Solomon, J., Perry, D., Sayre, P., Janosko, K.B., Lackemeyer, M.G., Bohannon, J.K., Kash, J.C., Jahrling, P.B., Taubenberger, J.K., 2016. Influenza A and methicillin-resistant Staphylococcus aureus co-infection in rhesus macaques - A model of severe pneumonia. Antiviral Res. 129, 120–129.

Cillóniz, C., Shinya, K., Peng, X., Korth, M.J., Proll, S.C., Aicher, L.D., Carter, V.S., Chang, J.H., Kobasa, D., Feldmann, F., Strong, J.E., Feldmann, H., Kawaoka, Y., Katze, M.G., 2009. Lethal influenza virus infection in macaques is associated with early dysregulation of inflammatory related genes. PLoS Pathog. 5.

CITES, 1973. Convention on International Trade in Endangered Species of Wild Fauna and Flora.

Clarke, C.J., Watt, N.J., Meredith, A., McIntyre, N., Burns, S.M., 1994. Respiratory syncytial virus-associated bronchopneumonia in a young chimpanzee. J. Comp. Pathol. 110, 207–212.

Cockrell, A.S., Yount, B.L., Scobey, T., Jensen, K., Douglas, M., Beall, A., Tang, X.C., Marasco, W.A., Heise, M.T., Baric, R.S., 2016. A mouse model for MERS coronavirus-induced acute respiratory distress syndrome. Nat. Microbiol. 2.

Coleman, M.T., Maiello, P., Tomko, J., Frye, L.J., Fillmore, D., Janssen, C., Klein, E., Lin, P.L., 2014. Early Changes by (18)Fluorodeoxyglucose positron emission tomography coregistered with computed tomography predict outcome after Mycobacterium tuberculosis infection in cynomolgus macaques. Infect. Immun. 82, 2400–2404.

Collins, P.L., Purcell, R.H., London, W.T., Lawrence, L.A., Chanock, R.M., Murphy, B.R., 1990. Evaluation in chimpanzees of vaccinia virus recombinants that express the surface glycoproteins of human respiratory syncytial virus. Vaccine 8, 164–168.

Cong, Y., Lentz, M.R., Lara, A., Alexander, I., Bartos, C., Bohannon, J.K., Hammoud, D., Huzella, L., Jahrling, P.B., Janosko, K., Jett, C., Kollins, E., Lackemeyer, M., Mollura, D., Ragland, D., Rojas, O., Solomon, J., Xu, Z., Munster, V., Holbrook, M.R., 2017. Loss in lung volume and changes in the immune response demonstrate disease progression in African green monkeys infected by small-particle aerosol and intratracheal exposure to Nipah virus. PLoS Negl. Trop. Dis. 11, e0005532.

Corbett, K.S., Flynn, B., Foulds, K.E., Francica, J.R., Boyoglu-Barnum, S., Werner, A.P., Flach, B., O'Connell, S., Bock, K.W., Minai, M., Nagata, B.M., Andersen, H., Martinez, D.R., Noe, A.T., Douek, N., Donaldson, M.M., Nji, N.N., Alvarado, G.S., Edwards, D.K., Flebbe, D.R., Lamb, E., Doria-Rose, N.A., Lin, B.C., Louder, M.K., O'Dell, S., Schmidt, S.D., Phung, E., Chang, L.A., Yap, C., Todd, J.M., Pessaint, L., Van Ry, A., Browne, S., Greenhouse, J., Putman-Taylor, T., Strasbaugh, A., Campbell, T.A., Cook, A., Dodson, A., Steingrebe, K., Shi, W., Zhang, Y., Abiona, O. M., Wang, L., Pegu, A., Yang, E.S., Leung, K., Zhou, T., Teng, I.T., Widge, A., Gordon, I., Novik, L., Gillespie, R.A., Loomis, R.J., Moliva, J.I., Stewart-Jones, G., Himansu, S., Kong, W.P., Nason, M.C., Morabito, K.M., Ruckwardt, T.J., Ledgerwood, J.E., Gaudinski, M.R., Kwong, P.D., Mascola, J.R., Carfi, A., Lewis, M. G., Baric, R.S., McDermott, A., Moore, I.N., Sullivan, N.J., Roederer, M., Seder, R.A., Graham, B.S., 2020. Evaluation of the mRNA-1273 vaccine against SARS-CoV-2 in nonhuman Primates. N. Engl. J. Med. 383, 1544–1555.

Cornelius, C.A., Quenee, L.E., Overheim, K.A., Koster, F., Brasel, T.L., Elli, D., Ciletti, N. A., Schneewind, O., 2008. Immunization with recombinant V10 protects cynomolgus macaques from lethal pneumonic plague. Infect. Immun. 76, 5588–5597.

Correia, B.E., Bates, J.T., Loomis, R.J., Baneyx, G., Carrico, C., Jardine, J.G., Rupert, P., Correnti, C., Kalyuzhniy, O., Vittal, V., Connell, M.J., Stevens, E., Schroeter, A., Chen, M., Macpherson, S., Serra, A.M., Adachi, Y., Holmes, M.A., Li, Y., Klevit, R.E.,

Graham, B.S., Wyatt, R.T., Baker, D., Strong, R.K., Crowe Jr., J.E., Johnson, P.R., Schief, W.R., 2014. Proof of principle for epitope-focused vaccine design. Nature 507, 201–206.

Criée, C.P., Sorichter, S., Smith, H.J., Kardos, P., Merget, R., Heise, D., Berdel, D., Köhler, D., Magnussen, H., Marek, W., Mitfessel, H., Rasche, K., Rolke, M., Worth, H., Jörres, R.A., 2011. Body plethysmography - its principles and clinical use. Respir. Med. 105, 959–971.

Cross, R.W., Agans, K.N., Prasad, A.N., Borisevich, V., Woolsey, C., Deer, D.J., Dobias, N. S., Geisbert, J.B., Fenton, K.A., Geisbert, T.W., 2020. Intranasal exposure of African green monkeys to SARS-CoV-2 results in acute phase pneumonia with shedding and lung injury still present in the early convalescence phase. Virol. J. 17, 125.

Crowe Jr., J.E., Collins, P.L., London, W.T., Chanock, R.M., Murphy, B.R., 1993. A comparison in chimpanzees of the immunogenicity and efficacy of live attenuated respiratory syncytial virus (RSV) temperature-sensitive mutant vaccines and vaccinia virus recombinants that express the surface glycoproteins of RSV. Vaccine 11, 1395–1404.

Culotta, C.S., Harvey, D.F., Gordon, E.F., 1935. Whooping cough. J. Pediatr. 6, 743–752.

Dabisch, P.A., Xu, Z., Boydston, J.A., Solomon, J., Bohannon, J.K., Yeager, J.J., Taylor, J. R., Reeder, R.J., Sayre, P., Seidel, J., Mollura, D.J., Hevey, M.C., Jahrling, P.B., Lackemeyer, M.G., 2017. Quantification of regional aerosol deposition patterns as a function of aerodynamic particle size in rhesus macaques using PET/CT imaging. Inhal. Toxicol. 29.

Davis, K.J., Fritz, D.L., Pitt, M.L., Welkos, S.L., Worsham, P.L., Friedlander, A.M., 1996. Pathology of experimental pneumonic plague produced by fraction 1-positive and fraction 1-negative Yersinia pestis in African green monkeys (Cercopithecus aethiops). Arch. Pathol. Lab. Med. 120, 156–163.

Davis, A.S., Taubenberger, J.K., Bray, M., 2015. The use of nonhuman primates in research on seasonal, pandemic and avian influenza, 1893-2014. Antiviral Res. 117, 75–98.

de Swart, R.L., Kuiken, T., Timmerman, H.H., Amerongen, Gv., van den Hoogen, B.G., Vos, H.W., Neijens, H.J., Andeweg, A.C., Osterhaus, A.D.M.E., 2002. Immunization of macaques with formalin-inactivated respiratory syncytial virus (RSV) induces Interleukin-13-Associated hypersensitivity to subsequent RSV infection. J. Virol. 76.

De Wit, E., Rasmussen, A.L., Falzarano, D., Bushmaker, T., Feldmann, F., Brining, D.L., Fischer, E.R., Martellaro, C., Okumura, A., Chang, J., Scott, D., Benecke, A.G., Katze, M.G., Feldmann, H., Munster, V.J., 2013. Middle East respiratory syndrome coronavirus (MERSCoV) causes transient lower respiratory tract infection in rhesus macaques. Proc. Natl. Acad. Sci. U.S.A. 110, 16598–16603.

DeMarco, G.J., Nunamaker, E.A., 2019. A review of the effects of pain and analgesia on immune system function and inflammation: relevance for preclinical studies. Comp. Med. 69, 520–534.

Deming, D., Sheahan, T., Heise, M., Yount, B., Davis, N., Sims, A., Suthar, M., Harkema, J., Whitmore, A., Pickles, R., West, A., Donaldson, E., Curtis, K., Johnston, R., Baric, R., 2006. Vaccine efficacy in senescent mice challenged with recombinant SARS-CoV bearing epidemic and zoonotic spike variants. PLoS Med. 3, 2359–2375.

Deng, W., Bao, L., Liu, J., Xiao, C., Liu, J., Xue, J., Lv, Q., Qi, F., Gao, H., Yu, P., Xu, Y., Qu, Y., Li, F., Xiang, Z., Yu, H., Gong, S., Liu, M., Wang, G., Wang, S., Song, Z., Liu, Y., Zhao, W., Han, Y., Zhao, L., Liu, X., Wei, Q., Qin, C., 2020a. Primary exposure to SARS-CoV-2 protects against reinfection in rhesus macaques. Science (New York, N.Y.) 369, 818–823.

Deng, W., Bao, L., Liu, J., Xiao, C., Liu, J., Xue, J., Lv, Q., Qi, F., Gao, H., Yu, P., Xu, Y., Qu, Y., Li, F., Xiang, Z., Yu, H., Gong, S., Liu, M., Wang, G., Wang, S., Song, Z., Liu, Y., Zhao, W., Han, Y., Zhao, L., Liu, X., Wei, Q., Qin, C., 2020b. Primary exposure to SARS-CoV-2 protects against reinfection in rhesus macaques. Science 369, 818–823.

Denoel, P., Philipp, M.T., Doyle, L., Martin, D., Carletti, G., Poolman, J.T., 2011. A protein-based pneumococcal vaccine protects rhesus macaques from pneumonia after experimental infection with Streptococcus pneumoniae. Vaccine 29, 5495–5501.

Diedrich, C.R., Mattila, J.T., Klein, E., Janssen, C., Phuah, J., Sturgeon, T.J., Montelaro, R.C., Lin, P.L., Flynn, J.L., 2010. Reactivation of latent tuberculosis in cynomolgus macaques infected with SIV is associated with early peripheral T cell depletion and not virus load. PLoS One 5 e9611-e9611.

Dijkman, K., Sombroek, C.C., Vervenne, R.A.W., Hofman, S.O., Boot, C., Remarque, E.J., Kocken, C.H.M., Ottenhoff, T.H.M., Kondova, I., Khayum, M.A., Haanstra, K.G., Vierboom, M.P.M., Verreck, F.A.W., 2019. Prevention of tuberculosis infection and disease by local BCG in repeatedly exposed rhesus macaques. Nat. Med. 25, 255–262.

Dubus, J.C., Vecellio, L., De Monte, M., Fink, J.B., Grimbert, D., Montharu, J., Valat, C., Behan, N., Diot, P., 2005. Aerosol deposition in neonatal ventilation. Pediatr. Res. 58.

Elahi, S., Brownlie, R., Korzeniowski, J., Buchanan, R., O'Connor, B., Peppler, M.S., Halperin, S.A., Lee, S.F., Babiuk, L.A., Gerdts, V., 2005. Infection of newborn piglets with Bordetella pertussis: a new model for pertussis. Infect. Immun. 73.

Elahi, S., Holmstrom, J., Gerdts, V., 2007. The benefits of using diverse animal models for studying pertussis. Trends Microbiol. 15, 462–468.

Falsey, A.R., Hennessey, P.A., Formica, M.A., Cox, C., Walsh, E.E., 2005. Respiratory syncytial virus infection in elderly and high-risk adults. N. Engl. J. Med. 352.

Finch, C.L., Crozier, I., Lee, J.H., Byrum, R., Cooper, T.K., Liang, J., Sharer, K., Solomon, J., Sayre, P.J., Kocher, G., Bartos, C., Aiosa, N.M., Castro, M., Larson, P.A., Adams, R., Beitzel, B., Di Paola, N., Kugelman, J.R., Kurtz, J.R., Burdette, T., Nason, M.C., Feuerstein, I.M., Palacios, G., Claire, M.C.S., Lackemeyer, M.G., Johnson, R.F., Braun, K.M., Ramuta, M.D., Wada, J., Schmaljohn, C.S., Friedrich, T. C., O'Connor, D.H., Kuhn, J.H., 2020. Characteristic and quantifiable COVID-19-like

abnormalities in CT- and PET/CT-imaged lungs of SARS-CoV-2-infected crab-eating macaques (&em&Macaca fascicularis&/em&). bioRxiv, 2020.2005.2014.096727.

Finegold, M.J., 1969. Pneumonic plague in monkeys. An electron microscopic study. Am. J. Pathol. 54, 167–185.

Fiole, D., Tournier, J.-N., 2016. Intravital microscopy of the lung: minimizing invasiveness. J. Biophotonics 9, 868–878.

Fiole, D., Deman, P., Trescos, Y., Mayol, J.-F., Mathieu, J., Vial, J.-C., Douady, J., Tournier, J.-N., 2014. Two-photon intravital imaging of lungs during anthrax infection reveals long-lasting macrophage-dendritic cell contacts. Infect. Immun. 82, 864–872.

Flynn, J.L., Gideon, H.P., Mattila, J.T., Lin, P.L., 2015. Immunology studies in non-human primate models of tuberculosis. Immunol. Rev. 264, 60–73.

Foreman, T.W., Mehra, S., LoBato, D.N., Malek, A., Alvarez, X., Golden, N.A., Bucşan, A. N., Didier, P.J., Doyle-Meyers, L.A., Russell-Lodrigue, K.E., Roy, C.J., Blanchard, J., Kuroda, M.J., Lackner, A.A., Chan, J., Khader, S.A., Jacobs Jr., W.R., Kaushal, D., 2016. CD4+ T-cell-independent mechanisms suppress reactivation of latent tuberculosis in a macaque model of HIV coinfection. Proc. Natl. Acad. Sci. U.S.A. 113, E5636–E5644.

Fouchier, R.A.M., Kuiken, T., Schutten, M., Van Amerongen, G., Van Doornum, G.J.J., Van Den Hoogen, B.G., Peiris, M., Lim, W., Stöhr, K., Osterhaus, A.D.M.E., 2003. Koch's postulates fulfilled for SARS virus. Nature 423, 240.

Fouchier, R.A.M., Hartwig, N.G., Bestebroer, T.M., Niemeyer, B., De Jong, J.C., Simon, J. H., Osterhaus, A.D.M.E., 2004. A previously undescribed coronavirus associated with respiratory disease in humans. Proc. Natl. Acad. Sci. U.S.A. 101, 6212–6216.

Freise, A.C., Wu, A.M., 2015. In vivo imaging with antibodies and engineered fragments. Mol. Immunol. 67, 142–152.

Glezen, W.P., 1986. Risk of primary infection and reinfection with respiratory syncytial virus. Arch. Pediatr. Adolesc. Med. 140.

Gorse, G.J., Patel, G.B., Vitale, J.N., O'Connor, T.Z., 2010. Prevalence of antibodies to four human coronaviruses is lower in nasal secretions than in serum. Clin. Vaccine Immunol. 17, 1875–1880.

Gowrishankar, G., Namavari, M., Jouannot, E.B., Hoehne, A., Reeves, R., Hardy, J., Gambhir, S.S., 2014. Investigation of 6-[18F]-fluoromaltose as a novel PET tracer for imaging bacterial infection. PLoS One 9, e107951.

Gretebeck, L.M., Subbarao, K., 2015. Animal models for SARS and MERS coronaviruses. Curr. Opin. Virol. 13, 123–129.

Grunwald, T., Tenbusch, M., Schulte, R., Raue, K., Wolf, H., Hannaman, D., de Swart, R. L., Uberla, K., Stahl-Hennig, C., 2014. Novel vaccine regimen elicits strong airway immune responses and control of respiratory syncytial virus in nonhuman Primates. J. Virol. 88.

Gu, J., Korteweg, C., 2007. Pathology and pathogenesis of severe acute respiratory syndrome. Am. J. Pathol. 170, 1136–1147.

Gupta, N., Kumar, R., Agrawal, B., 2018. New players in immunity to tuberculosis: the host microbiome, lung epithelium, and innate immune cells. Front. Immunol. 9, 709.

Gupta, A., Madhavan, M.V., Sehgal, K., Nair, N., Mahajan, S., Sehrawat, T.S., Bikdeli, B., Ahluwalia, N., Ausiello, J.C., Wan, E.Y., Freedberg, D.E., Kirtane, A.J., Parikh, S.A., Maurer, M.S., Nordvig, A.S., Accili, D., Bathon, J.M., Mohan, S., Bauer, K.A., Leon, M.B., Krumholz, H.M., Uriel, N., Mehra, M.R., Elkind, M.S.V., Stone, G.W., Schwartz, A., Ho, D.D., Bilezikian, J.P., Landry, D.W., 2020. Extrapulmonary manifestations of COVID-19. Nat. Med. 26, 1017–1032.

Haagmans, B.L., van den Brand, J.M.A., Provacia, L.B., Raj, V.S., Stittelaar, K.J., Getu, S., de Waal, L., Bestebroer, T.M., van Amerongen, G., Verjans, G.M.G.M., Fouchier, R.A. M., Smits, S.L., Kuiken, T., Osterhaus, A.D.M.E., 2015. Asymptomatic middle east respiratory syndrome coronavirus infection in rabbits. J. Virol. 89, 6131–6135.

Habibi, M.S., Jozwik, A., Makris, S., Dunning, J., Paras, A., DeVincenzo, J.P., De Haan, C. A.M., Wrammert, J., Openshaw, P.J.M., Chiu, C., 2015. Impaired antibody-mediated protection and defective iga b-cell memory in experimental infection of adults with respiratory syncytial virus. Am. J. Respir. Crit. Care Med. 191, 1040–1049.

Hall, C.B., Long, C.E., Schnabel, K.C., 2001. Respiratory syncytial virus infections in previously healthy working adults. Clin. Infect. Dis. 33.

Hammoud, D.A., Lentz, M.R., Lara, A., Bohannon, J.K., Feuerstein, I., Huzella, L., Jahrling, P.B., Lackemeyer, M., Laux, J., Rojas, O., Sayre, P., Solomon, J., Cong, Y., Munster, V., Holbrook, M.R., 2018. Aerosol exposure to intermediate size Nipah virus particles induces neurological disease in African green monkeys. PLoS Negl. Trop. Dis. 12, e0006978.

Harkema, J.R., 1991. Comparative aspects of nasal airway anatomy: relevance to inhalation toxicology ^{*1}. Toxicol. Pathol. 19.

Hartings, J.M., Roy, C.J., 2004. The automated bioaerosol exposure system: preclinical platform development and a respiratory dosimetry application with nonhuman primates. J. Pharmacol. Toxicol. Methods 49, 39–55.

Hartman, A.L., Nambulli, S., McMillen, C.M., White, A.G., Tilston-Lunel, N.L., Albe, J.R., Cottle, E., Dunn, M.D., Frye, L.J., Gilliland, T.H., Olsen, E.L., O'Malley, K.J., Schwarz, M.M., Tomko, J.A., Walker, R.C., Xia, M., Hartman, M.S., Klein, E., Scanga, C.A., Flynn, J.L., Klimstra, W.B., McElroy, A.K., Reed, D.S., Duprex, W.P., 2020. SARS-CoV-2 infection of African green monkeys results in mild respiratory disease discernible by PET/CT imaging and shedding of infectious virus from both respiratory and gastrointestinal tracts. PLoS Pathog. 16.

Heberling, R.L., Kalter, S.S., 1970. Persistence and spread of influenza virus (A2-Hong Kong) in normal and poly I.C. Treated baboons (Papio cynocephalus). Proc. Soc. Exp. Biol. Med. 135, 717–723.

Hogg, J.C., 2004. Pathophysiology of airflow limitation in chronic obstructive pulmonary disease. Lancet 364, 709–721.

Honko, A.N., Sriranganathan, N., Lees, C.J., Mizel, S.B., 2006. Flagellin is an effective adjuvant for immunization against lethal respiratory challenge with Yersinia pestis. Infect. Immun. 74, 1113–1120.

Huang, D., Chen, C.Y., Ali, Z., Shao, L., Shen, L., Lockman, H.A., Barnewall, R.E., Sabourin, C., Eestep, J., Reichenberg, A., Hintz, M., Jomaa, H., Wang, R., Chen, Z.W., 2009. Antigen-specific Vgamma2Vdelta2 T effector cells confer homeostatic protection against pneumonic plaque lesions. Proc. Natl. Acad. Sci. U.S.A. 106, 7553–7558.

Huang, D., Chen, C.Y., Zhang, M., Qiu, L., Shen, Y., Du, G., Zhou, K., Wang, R., Chen, Z. W., 2012. Clonal Immune Responses of Mycobacterium-Specific γδ T Cells in Tuberculous and Non-Tuberculous Tissues during M. tuberculosis Infection. PLoS One 7, e30631.

Imai, M., Iwatsuki-Horimoto, K., Hatta, M., Loeber, S., Halfmann, P.J., Nakajima, N., Watanabe, T., Ujie, M., Takahashi, K., Ito, M., Yamada, S., Fan, S., Chiba, S., Kuroda, M., Guan, L., Takada, K., Armbrust, T., Balogh, A., Furusawa, Y., Okuda, M., Ueki, H., Yasuhara, A., Sakai-Tagawa, Y., Lopes, T.J.S., Kiso, M., Yamayoshi, S., Kinoshita, N., Ohmagari, N., Hattori, S.I., Takeda, M., Mitsuya, H., Krammer, F., Suzuki, T., Kawaoka, Y., 2020. Syrian hamsters as a small animal model for SARS-CoV-2 infection and countermeasure development. Proc. Natl. Acad. Sci. U.S.A. 117, 16587–16595.

Irwin, M.R., Cole, S.W., 2011. Reciprocal regulation of the neural and innate immune systems. Nat. Rev. Immunol. 11, 625–632.

ISO, 2013. Anaesthetic and Respiratory Equipment — Nebulizing Systems and Components. ISO. iso.org.

Janis, E., Kaufmann, S., Schwartz, R., Pardoll, D., 1989. Activation of gamma delta T cells in the primary immune response to Mycobacterium tuberculosis. Science 244, 713–716.

Jegaskanda, S., Amarasena, T.H., Laurie, K.L., Tan, H.X., Butler, J., Parsons, M.S., Alcantara, S., Petravic, J., Davenport, M.P., Hurt, A.C., Reading, P.C., Kent, S.J., 2013. Standard trivalent influenza virus protein vaccination does not prime antibody-dependent cellular cytotoxicity in macaques. J. Virol. 87, 13706–13718.

Jia, W., Channappanavar, R., Zhang, C., Li, M., Zhou, H., Zhang, S., Zhou, P., Xu, J., Shan, S., Shi, X., Wang, X., Zhao, J., Zhou, D., Perlman, S., Zhang, L., 2019. Single intranasal immunization with chimpanzee adenovirus-based vaccine induces sustained and protective immunity against MERS-CoV infection. Emerg. Microbes Infect. 8, 760–772.

Jones, B.G., Sealy, R.E., Rudraraju, R., Traina-Dorge, V.L., Finneyfrock, B., Cook, A., Takimoto, T., Portner, A., Hurwitz, J.L., 2012. Sendai virus-based RSV vaccine protects African green monkeys from RSV infection. Vaccine 30.

Judge, E.P., Hughes, J.M., Egan, J.J., Maguire, M., Molloy, E.L., O'Dea, S., 2014. Anatomy and bronchoscopy of the porcine lung. A model for translational respiratory medicine. Am. J. Respir. Cell Mol. Biol. 51, 334–343.

Kakuk, T.J., Soike, K., Brideau, R.J., Zaya, R.M., Cole, S.L., Zhang, J.Y., Roberts, E.D., Wells, P.A., Wathen, M.W., 1993. A human respiratory syncytial virus (RSV) primate model of enhanced pulmonary pathology induced with a formalin-inactivated RSV vaccine but not a recombinant FG subunit vaccine. J. Infect. Dis. 167.

Kapil, P., Papin, J.F., Wolf, R.F., Zimmerman, L.I., Wagner, L.D., Merkel, T.J., 2018. Maternal vaccination with a monocomponent pertussis toxoid vaccine is sufficient to protect infants in a baboon model of whooping cough. J. Infect. Dis. 217, 1231–1236.

Kaushal, D., Mehra, S., Didier, P.J., Lackner, A.A., 2012. The non-human primate model of tuberculosis. J. Med. Primatol. 41, 191–201.

Kim, H.W., Canchola, J.G., Brandt, C.D., Pyles, G., Chanock, R.M., Jensen, K., Parrott, R. H., 1969. Respiratory syncytial virus disease in infants despite prior administration of antigenic inactivated VACCINE12. Am. J. Epidemiol. 89.

Kim, M.H., Kim, H.J., Chang, J., 2019. Superior immune responses induced by intranasal immunization with recombinant adenovirus-based vaccine expressing fulllength Spike protein of Middle East respiratory syndrome coronavirus. PLoS One 14.

Kim, Y.-I., Kim, S.-G., Kim, S.-M., Kim, E.-H., Park, S.-J., Yu, K.-M., Chang, J.-H., Kim, E. J., Lee, S., Casel, M.A.B., Um, J., Song, M.-S., Jeong, H.W., Lai, V.D., Kim, Y., Chin, B. S., Park, J.-S., Chung, K.-H., Foo, S.-S., Poo, H., Mo, I.-P., Lee, O.-J., Webby, R.J., Jung, J.U., Choi, Y.K., 2020. Infection and rapid transmission of SARS-CoV-2 in ferrets. Cell Host Microbe.

Kitano, M., Itoh, Y., Kodama, M., Ishigaki, H., Nakayama, M., Nagata, T., Ishida, H., Tsuchiya, H., Torii, R., Baba, K., Yoshida, R., Sato, A., Ogasawara, K., 2010. Establishment of a cynomolgus macaque model of influenza B virus infection. Virology 407, 178–184.

Kitano, M., Itoh, Y., Kodama, M., Ishigaki, H., Nakayama, M., Ishida, H., Baba, K., Noda, T., Sato, K., Nihashi, Y., Kanazu, T., Yoshida, R., Torii, R., Sato, A., Ogasawara, K., 2011. Efficacy of single intravenous injection of peramivir against influenza B virus infection in ferrets and cynomolgus macaques. Antimicrob. Agents Chemother. 55, 4961–4970.

Kobayashi, S.D., Olsen, R.J., LaCasse, R.A., Safronetz, D., Ashraf, M., Porter, A.R., Braughton, K.R., Feldmann, F., Clifton, D.R., Kash, J.C., Bailey, J.R., Gardner, D.J., Otto, M., Brining, D.L., Kreiswirth, B.N., Taubenberger, J.K., Parnell, M.J., Feldmann, H., Musser, J.M., DeLeo, F.R., 2013. Seasonal H3N2 influenza A virus fails to enhance Staphylococcus aureus co-infection in a non-human primate respiratory tract infection model. Virulence 4, 707–715.

Koster, F., Perlin, D.S., Park, S., Brasel, T., Gigliotti, A., Barr, E., Myers, L., Layton, R.C., Sherwood, R., Lyons, C.R., 2010. Milestones in progression of primary pneumonic plague in cynomolgus macaques. Infect. Immun. 78, 2946–2955.

Kuiken, T., Fouchier, R.A.M., Schutten, M., Rimmelzwaan, G.F., Van Amerongen, G., Van Riel, D., Laman, J.D., De Jong, T., Van Doornum, G., Lim, W., Ling, A.E., Chan, P.K. S., Tam, J.S., Zambon, M.C., Gopal, R., Drosten, C., Van Der Werf, S., Escriou, N., Manuguerra, J.C., Stöhr, K., Peiris, J.S.M., Osterhaus, A.D.M.E., 2003. Newly discovered coronavirus as the primary cause of severe acute respiratory syndrome. Lancet 362, 263–270.

Kulkarni, P., Qi, C., Fukushima, N., 2016. Development of portable aerosol mobility spectrometer for personal and mobile aerosol measurement. Aerosol Sci Tech. 50, 1167–1179.

Larios Mora, A., Detalle, L., Van Geelen, A., Davis, M.S., Stohr, T., Gallup, J.M., Ackermann, M.R., 2015. Kinetics of respiratory syncytial virus (RSV) Memphis strain 37 (M37) infection in the respiratory tract of newborn lambs as an RSV infection model for human infants. PLoS One 10.

Layton, R.C., Brasel, T., Gigliotti, A., Barr, E., Storch, S., Myers, L., Hobbs, C., Koster, F., 2011. Primary pneumonic plague in the African Green monkey as a model for treatment efficacy evaluation. J. Med. Primatol. 40, 6–17.

Lee, N., Lui, G.C.Y., Wong, K.T., Li, T.C.M., Tse, E.C.M., Chan, J.Y.C., Yu, J., Wong, S.S. M., Choi, K.W., Wong, R.Y.K., Ngai, K.L.K., Hui, D.S.C., Chan, P.K.S., 2013. High morbidity and mortality in adults hospitalized for respiratory syncytial virus infections. Clin. Infect. Dis. 57.

Lee, J.H., Hammoud, D.A., Cong, Y., Huzella, L.M., Castro, M.A., Solomon, J., Laux, J., Lackemeyer, M., Bohannon, J.K., Rojas, O., Byrum, R., Adams, R., Ragland, D., St Claire, M., Munster, V., Holbrook, M.R., 2020. The use of large-particle aerosol exposure to nipah virus to mimic human neurological disease manifestations in the african green monkey. J. Infect. Dis. 221, S419–S430.

Li, K., Wohlford-Lenane, C.L., Channappanavar, R., Park, J.E., Earnest, J.T., Bair, T.B., Bates, A.M., Brogden, K.A., Flaherty, H.A., Gallagher, T., Meyerholz, D.K., Perlman, S., McCray, P.B., 2017. Mouse-adapted MERS coronavirus causes lethal lung disease in human DPP4 knockin mice. Proc. Natl. Acad. Sci. U.S.A. 114, E3119–E3128.

Limited, P., 2017. Feasibility Study As Required in Article 10 of Directive 2010/63/EU on the Protection of Animals Used for Scientific Purposes.

Lin, P.L., Flynn, J.L., 2018. The end of the binary era: revisiting the Spectrum of tuberculosis. J. Immunol. 201, 2541-LP - 2548.

Lin, P.L., Rodgers, M., Smith, Lk., Bigbee, M., Myers, A., Bigbee, C., Chiosea, I., Capuano, S.V., Fuhrman, C., Klein, E., Flynn, J.L., 2009. Quantitative comparison of active and latent tuberculosis in the cynomolgus macaque model. Infect. Immun. 77, 4631–4642.

Lin, P.L., Coleman, T., Carney, J.P.J., Lopresti, B.J., Tomko, J., Fillmore, D., Dartois, V., Scanga, C., Frye, L.J., Janssen, C., Klein, E., Barry 3rd, C.E., Flynn, J.L., 2013a. Radiologic responses in Cynomolgus macaques for assessing tuberculosis chemotherapy regimens. Antimicrob. Agents Chemother. 57, 4237–4244.

Lin, P.L., Coleman, T., Carney, J.P.J., Lopresti, B.J., Tomko, J., Fillmore, D., Dartois, V., Scanga, C., Frye, L.J., Janssen, C., Klein, E., Barry, C.E., Flynn, J.L., 2013b. Radiologic responses in Cynomolgus macaques for assessing tuberculosis chemotherapy regimens. Antimicrob. Agents Chemother. 57, 4237–4244.

Lin, P.L., Ford, C.B., Coleman, M.T., Myers, A.J., Gawande, R., Ioerger, T., Sacchettini, J., Fortune, S.M., Flynn, J.L., 2014. Sterilization of granulomas is common in active and latent tuberculosis despite within-host variability in bacterial killing. Nat. Med. 20, 75–79.

Liu, L., Wei, Q., Lin, Q., Fang, J., Wang, H., Kwok, H., Tang, H., Nishiura, K., Peng, J., Tan, Z., Wu, T., Cheung, K.W., Chan, K.H., Alvarez, X., Qin, C., Lackner, A., Perlman, S., Yuen, K.Y., Chen, Z., 2019. Anti-spike IgG causes severe acute lung injury by skewing macrophage responses during acute SARS-CoV infection. JCI Insight 4.

Locht, C., Papin, J.F., Lecher, S., Debrie, A.-S., Thalen, M., Solovay, K., Rubin, K., Mielcarek, N., 2017. Live attenuated pertussis vaccine BPZE1 protects baboons against B. Pertussis disease and infection. J. Infect. Dis.

Lu, S., Zhao, Y., Yu, W., Yang, Y., Gao, J., Wang, J., Kuang, D., Yang, M., Yang, J., Ma, C., Xu, J., Qian, X., Li, H., Zhao, S., Li, J., Wang, H., Long, H., Zhou, J., Luo, F., Ding, K., Wu, D., Zhang, Y., Dong, Y., Liu, Y., Zheng, Y., Lin, X., Jiao, L., Zheng, H., Dai, Q., Sun, Q., Hu, Y., Ke, C., Liu, H., Peng, X., 2020. Comparison of nonhuman primates identified the suitable model for COVID-19. Signal Transduct. Target. Ther. 5.

Maiello, P., DiFazio, R.M., Cadena, A.M., Rodgers, M.A., Lin, P.L., Scanga, C.A., Flynn, J. L., 2018. Rhesus macaques are more susceptible to progressive tuberculosis than Cynomolgus macaques: a quantitative comparison. Infect. Immun. 86, e00505–00517.

Maisonnasse, P., Guedj, J., Contreras, V., Behillil, S., Solas, C., Marlin, R., Naninck, T., Pizzorno, A., Lemaitre, J., Gonçalves, A., Kahlaoui, N., Terrier, O., Fang, R.H.T., Enouf, V., Dereuddre-Bosquet, N., Brisebarre, A., Touret, F., Chapon, C., Hoen, B., Lina, B., Calatrava, M.R., van der Werf, S., de Lamballerie, X., Le Grand, R., 2020. Hydroxychloroquine use against SARS-CoV-2 infection in non-human primates. Nature 585, 584–587.

Malachowa, N., Kobayashi, S.D., Porter, A.R., Freedman, B., Hanley, P.W., Lovaglio, J., Saturday, G.A., Gardner, D.J., Scott, D.P., Griffin, A., Cordova, K., Long, D., Rosenke, R., Sturdevant, D.E., Bruno, D., Martens, C., Kreiswirth, B.N., DeLeo, F.R., 2019. Vaccine protection against multidrug-resistant Klebsiella pneumoniae in a nonhuman primate model of severe lower respiratory tract infection. mBio 10.

Marcandalli, J., Fiala, B., Ols, S., Perotti, M., de van der Schueren, W., Snijder, J., Hodge, E., Benhaim, M., Ravichandran, R., Carter, L., Sheffler, W., Brunner, L., Lawrenz, M., Dubois, P., Lanzavecchia, A., Sallusto, F., Lee, K.K., Veesler, D., Correnti, C.E., Stewart, L.J., Baker, D., Loré, K., Perez, L., King, N.P., 2019. Induction of potent neutralizing antibody responses by a designed protein nanoparticle vaccine for respiratory syncytial virus. Cell 176.

Margine, I., Krammer, F., 2014. Animal models for influenza viruses: implications for universal vaccine development. Pathogens 3, 846–874.

Masopust, D., Sivula, C.P., Jameson, S.C., 2017. Of mice, dirty mice, and men: using mice to understand human immunology. J. Immunol. 199, 383–388.

Mathieu, A., Guillon, A., Leyre, S., Martin, F., Fusciardi, J., Laffon, M., 2013. Aerosolized lidocaine during invasive mechanical ventilation: in vitro characterization and clinical efficiency to prevent systemic and cerebral hemodynamic changes induced

by endotracheal suctioning in head-injured patients. J. Neurosurg. Anesthesiol. 25, 8–15.

McArthur-Vaughan, K., Gershwin, L.J., 2002. A rhesus monkey model of respiratory syncytial virus infection. J. Med. Primatol. 31.

McAuliffe, J., Vogel, L., Roberts, A., Fahle, G., Fischer, S., Shieh, W.J., Butler, E., Zaki, S., St. Claire, M., Murphy, B., Subbarao, K., 2004. Replication of SARS coronavirus administered into the respiratory tract of African Green, rhesus and cynomolgus monkeys. Virology 330, 8–15.

McCray, P.B., Pewe, L., Wohlford-Lenane, C., Hickey, M., Manzel, L., Shi, L., Netland, J., Jia, H.P., Halabi, C., Sigmund, C.D., Meyerholz, D.K., Kirby, P., Look, D.C., Perlman, S., 2007. Lethal infection of K18-hACE2 mice infected with severe acute respiratory syndrome coronavirus. J. Virol. 81, 813–821.

McCullers, J.A., Tuomanen, E.I., 2001. Molecular pathogenesis of pneumococcal pneumonia. Front Biosci 6, D877–889.

McIntosh, K., Perlman, S., 2015. Coronaviruses, including severe acute respiratory syndrome (SARS) and Middle East respiratory syndrome (MERS). Mandell, Douglas, and Bennett's Principles and Practice of Infectious Diseases, pp. 1928–1936 e1922.

McIntosh, K., Dees, J.H., Becker, W.B., Kapikian, A.Z., Chanock, R.M., 1967. Recovery in tracheal organ cultures of novel viruses from patients with respiratory disease. Proc. Natl. Acad. Sci. U.S.A. 57, 933–940.

Merkel, T.J., Halperin, S.A., 2014. Nonhuman primate and human challenge models of pertussis. J. Infect. Dis. 209 (Suppl 1), S20–23.

Miller, L.A., Royer, C.M., Pinkerton, K.E., Schelegle, E.S., 2017. Nonhuman primate models of respiratory disease: past, present, and future. ILAR J. 58, 269–280.

Miyake, T., Soda, K., Itoh, Y., Sakoda, Y., Ishigaki, H., Nagata, T., Ishida, H., Nakayama, M., Ozaki, H., Tsuchiya, H., Torii, R., Kida, H., Ogasawara, K., 2010. Amelioration of pneumonia with Streptococcus pneumoniae infection by inoculation with a vaccine against highly pathogenic avian influenza virus in a non-human primate mixed infection model. J. Med. Primatol. 39, 58–70.

Mooij, P., Mortier, D., Stammes, M., Fagrouch, Z., Verschoor, E.J., Bogers, W., Koopman, G., 2020. Aerosolized pH1N1 influenza infection induces less systemic and local immune activation in the lung than combined intrabronchial, nasal and oral exposure in cynomolgus macaques. J. Gen. Virol. 101, 1229–1241.

Mooij, P., Stammes, M.A., Mortier, D., Fagrouch, Z., van Driel, N., Verschoor, E.J., Kondova, I., Bogers, W., Koopman, G., 2021. Aerosolized exposure to H5N1 influenza virus causes less severe disease than infection via combined intrabronchial, oral, and nasal inoculation in Cynomolgus macaques. Viruses 13.

Moran, et al., 2006. Methicillin-resistant S. aureus infections among patients in the emergency department. N. Engl. J. Med. 355 (7), 666–674. https://doi.org/10.1056/NEJMoa055356.

Morris, J.A., Blount, R.E., Savage, R.E., 1956. Recovery of cytopathogenic agent from chimpanzees with goryza. Exp. Biol. Med. 92.

Muñoz-Fontela, C., Dowling, W.E., Funnell, S.G.P., Gsell, P.S., Riveros-Balta, A.X., Albrecht, R.A., Andersen, H., Baric, R.S., Carroll, M.W., Cavaleri, M., Qin, C., Crozier, I., Dallmeier, K., de Waal, L., de Wit, E., Delang, L., Dohm, E., Duprex, W.P., Falzarano, D., Finch, C.L., Frieman, M.B., Graham, B.S., Gralinski, L.E., Guilfoyle, K., Haagmans, B.L., Hamilton, G.A., Hartman, A.L., Herfst, S., Kaptein, S.J.F., Klimstra, W.B., Knezevic, I., Krause, P.R., Kuhn, J.H., Le Grand, R., Lewis, M.G., Liu, W.C., Maisonnasse, P., McElroy, A.K., Munster, V., Oreshkova, N., Rasmussen, A.L., Rocha-Pereira, J., Rockx, B., Rodríguez, E., Rogers, T.F., Salguero, F.J., Schotsaert, M., Stittelaar, K.J., Thibaut, H.J., Tseng, C.T., Vergara-Alert, J., Beer, M., Brasel, T., Chan, J.F.W., García-Sastre, A., Neyts, J., Perlman, S., Reed, D.S., Richt, J.A., Roy, C.J., Segalés, J., Vasan, S.S., Henao-Restrepo, A.M., Barouch, D.H., 2020. Animal models for COVID-19. Nature 586, 509–515.

Munoz-Price, L.S., Poirel, L., Bonomo, R.A., Schwaber, M.J., Daikos, G.L., Cormican, M., Cornaglia, G., Garau, J., Gniadkowski, M., Hayden, M.K., Kumarasamy, K., Livermore, D.M., Maya, J.J., Nordmann, P., Patel, J.B., Paterson, D.L., Pitout, J., Villegas, M.V., Wang, H., Woodford, N., Quinn, J.P., 2013. Clinical epidemiology of the global expansion of Klebsiella pneumoniae carbapenemases. Lancet Infect. Dis. 13, 785–796.

Munster, V.J., de Wit, E., Feldmann, H., 2013. Pneumonia from human coronavirus in a macaque model. N. Engl. J. Med. 368, 1560–1562.

Munster, V.J., Feldmann, F., Williamson, B.N., van Doremalen, N., Pérez-Pérez, L., Schulz, J., Meade-White, K., Okumura, A., Callison, J., Brumbaugh B., Avanzato, V. A., Rosenke, R., Hanley, P.W., Saturday, G., Scott, D., Fischer, E.R., de Wit, E., 2020. Respiratory disease in rhesus macaques inoculated with SARS-CoV-2. Nature 585, 268–272.

Naninck, T., Coutte, L., Mayet, C., Contreras, V., Locht, C., Le Grand, R., Chapon, C., 2018. In vivo imaging of bacterial colonization of the lower respiratory tract in a baboon model of Bordetella pertussis infection and transmission. Sci. Rep. 8, 12297.

NC3Rs, 2017. Non-human Primate Accommodation, Care and Use.

NEAVS, 2021. International Bans | Laws | Release & Restitution for Chimpanzees.

Nelson, S., Happel, K.I., Zhang, P., Myers, L., Dufour, J.P., Bagby, G.J., 2013. Effect of bacterial pneumonia on lung simian immunodeficiency virus (SIV) replication in alcohol consuming SIV-infected rhesus macaques. Alcohol. Clin. Exp. Res. 37, 969–977.

Nicholls, J.M., Poon, L.L.M., Lee, K.C., Ng, W.F., Lai, S.T., Leung, C.Y., Chu, C.M., Hui, P. K., Mak, K.L., Lim, W., Yan, K.W., Chan, K.H., Tsang, N.C., Guan, Y., Yuen, K.Y., Peiris, J.S.M., 2003. Lung pathology of fatal severe acute respiratory syndrome. Lancet 361, 1773–1778.

NIH, 2015. NIH Will No Longer Support Biomedical Research on Chimpanzees | National Institutes of Health (NIH). National Institutes of Health.

Obot Akata, C.J., Blair, L.F., Barr, E.B., Storch, S., Vigil, G., Campen, M.J., 2007. Development of a head-out plethysmograph system for non-human primates in an Animal Biosafety Level 3 facility. J. Pharmacol. Toxicol. Methods 55, 96–102.

Olsen, R.J., Ashraf, M., Gonulal, V.E., Ayeras, A.A., Cantu, C., Shea, P.R., Carroll, R.K., Humbird, T., Greaver, J.L., Swain, J.L., Chang, E., Ragasa, W., Jenkins, L., Lally, K. P., Blasdel, T., Cagle, P., Musser, J.M., 2010a. Lower respiratory tract infection in cynomolgus macaques (Macaca fascicularis) infected with group A Streptococcus. Microb. Pathog. 49, 336–347.

Olsen, R.J., Kobayashi, S.D., Ayeras, A.A., Ashraf, M., Graves, S.F., Ragasa, W., Humbird, T., Greaver, J.L., Cantu, C., Swain, J.L., Jenkins, L., Blasdel, T., Cagle, P.T., Gardner, D.J., DeLeo, F.R., Musser, J.M., 2010b. Lack of a major role of Staphylococcus aureus Panton-Valentine leukocidin in lower respiratory tract infection in nonhuman primates. Am. J. Pathol. 176, 1346–1354.

Osterhaus, A.D.M.E., Fouchier, R.A.M., Kuiken, T., 2004. The aetiology of SARS: koch's postulates fulfilled. Royal Society 1081–1082.

Padro, C.J., Sanders, V.M., 2014. Neuroendocrine regulation of inflammation. Semin. Immunol. 26, 357–368.

Papin, J.F., Wolf, R.F., Kosanke, S.D., Jenkins, J.D., Moore, S.N., Anderson, M.P., Welliver, R.C., 2013. Infant baboons infected with respiratory syncytial virus develop clinical and pathological changes that parallel those of human infants. Am. J. Physiol-Lung Cell. Mol, Physiol. 304.

Paquin-Proulx, D., Costa, P.R., Terrassani Silveira, C.G., Marmorato, M.P., Cerqueira, N. B., Sutton, M.S., O'Connor, S.L., Carvalho, K.I., Nixon, D.F., Kallas, E.G., 2018. Latent Mycobacterium tuberculosis infection is associated with a higher frequency of mucosal-associated invariant t and invariant natural killer t cells. Front. Immunol. 9, 1394.

Parent, 2015. Comparative Biology of the Normal Lung. Elsevier.

Patra, A.L., 1986. Comparative anatomy of mammalian respiratory tracts: the nasopharyngeal region and the tracheobronchial region. J. Toxicol. Environ. Health 17.

Patton, K., Aslam, S., Shambaugh, C., Lin, R., Heeke, D., Frantz, C., Zuo, F., Esser, M.T., Paliard, X., Lambert, S.L., 2015. Enhanced immunogenicity of a respiratory syncytial virus (RSV) F subunit vaccine formulated with the adjuvant GLA-SE in cynomolgus macaques. Vaccine 33.

Peiris, J.S.M., Chu, C.M., Cheng, V.C.C., Chan, K.S., Hung, I.F.N., Poon, L.L.M., Law, K.I., Tang, B.S.F., Hon, T.Y.W., Chan, C.S., Chan, K.H., Ng, J.S.C., Zheng, B.J., Ng, W.L., Lai, R.W.M., Guan, Y., Yuen, K.Y., 2003. Clinical progression and viral load in a community outbreak of coronavirus-associated SARS pneumonia: a prospective study. Lancet 361, 1767–1772.

Peiris, J.S.M., Guan, Y., Yuen, K.Y., 2004. Severe acute respiratory syndrome. Nat. Med. 10, S88–S97.

Peña, J.C., Ho, W.-Z., 2015. Monkey models of tuberculosis: lessons learned. Infect. Immun. 83, 852–862.

Perry, R.D., Fetherston, J.D., 1997. Yersinia pestis–etiologic agent of plague. Clin. Microbiol. Rev. 10, 35–66.

Philipp, M.T., Purcell, J.E., Martin, D.S., Buck, W.R., Plauche, G.B., Ribka, E.P., DeNoel, P., Hermand, P., Leiva, L.E., Bagby, G.J., Nelson, S., 2006. Experimental infection of rhesus macaques with Streptococcus pneumoniae: a possible model for vaccine assessment. J. Med. Primatol. 35, 113–122.

Philipp, M.T., Doyle, L.A., Martin, D.S., Plauche, G.B., Phillippi-Falkenstein, K.M., Bohm Jr., R.P., 2012. A rhesus macaque model of Streptococcus pneumoniae carriage. J. Med. Primatol. 41, 60–66.

Plopper, C., Harkema, J., 2005. The Respiratory System and Its Use in Research, pp. 503–526.

Ponnuraj, E.M., Hayward, A.R., Raj, A., Wilson, H., Simoes, E.A.F., 2001. Increased replication of respiratory syncytial virus (RSV) in pulmonary infiltrates is associated with enhanced histopathological disease in bonnet monkeys (Macaca radiata) pre-immunized with a formalin-inactivated RSV vaccine. J. Gen. Virol. 82.

Prince, G.A., Bennett Jenson, A., Horswood, R.L., Camargo, E., Chanock, R.M., 1978. The pathogenesis of respiratory syncytial virus infection in cotton rats. Am. J. Pathol. 93, 771–791.

Prince, G.A., Suffin, S.C., Prevar, D.A., Camargo, E., Sly, D.L., London, W.T., Chanock, R. M., 1979. Respiratory syncytial virus infection in owl monkeys: viral shedding, immunological response, and associated illness caused by wild-type virus and two temperature-sensitive mutants. Infect. Immun. 26.

Puelles, V.G., Lütgehetmann, M., Lindenmeyer, M.T., Sperhake, J.P., Wong, M.N., Allweiss, L., Chilla, S., Heinemann, A., Wanner, N., Liu, S., Braun, F., Lu, S., Pfefferle, S., Schröder, A.S., Edler, C., Gross, O., Glatzel, M., Wichmann, D., Wiech, T., Kluge, S., Pueschel, K., Aepfelbacher, M., Huber, T.B., 2020. Multiorgan and renal tropism of SARS-CoV-2. N. Engl. J. Med. 383, 590–592.

Ram, J., Pineda-Cely, J., Calhoun, W.J., 2019. Forced oscillometry: a new tool for assessing airway function—is it ready for prime time? J. Allergy Clin. Immunol. Pract. 7, 2861–2862.

Remmers, J.E., 1976. Analysis of ventilatory response. Chest 70, 134–137.

Reyes, L.F., Restrepo, M.I., Hinojosa, C.A., Soni, N.J., Anzueto, A., Babu, B.L., Gonzalez-Juarbe, N., Rodriguez, A.H., Jimenez, A., Chalmers, J.D., Aliberti, S., Sibila, O., Winter, V.T., Coalson, J.J., Giavedoni, L.D., Dela Cruz, C.S., Waterer, G.W., Witzenrath, M., Suttorp, N., Dube, P.H., Orihuela, C.J., 2017. Severe pneumococcal pneumonia causes acute cardiac toxicity and subsequent cardiac remodeling. Am. J. Respir. Crit. Care Med. 196, 609–620.

Rich, A.R., Long, P.H., Brown, J.H., Bliss, E.A., Holt, L.E., 1932. Experiments upon the cause of whooping cough. Science 76, 330–331.

Richardson, L.S., Belshe, R.B., Sly, D.L., London, W.T., Prevar, D.A., Camargo, E., Chanock, R.M., 1978. Experimental respiratory syncytial virus pneumonia in cebus monkeys. J. Med. Virol. 2.

Roberts, A., Paddock, C., Vogel, L., Butler, E., Zaki, S., Subbarao, K., 2005. Aged BALB/c mice as a model for increased severity of severe acute respiratory syndrome in elderly humans. J. Virol. 79, 5833–5838.

Roberts, A., Deming, D., Paddock, C.D., Cheng, A., Yount, B., Vogel, L., Herman, B.D., Sheahan, T., Heise, M., Genrich, G.L., Zaki, S.R., Baric, R., Subbarao, K., 2007. A mouse-adapted SARS-coronavirus causes disease and mortality in BALB/c mice. PLoS Pathog. 3, 0023–0037.

Rockx, B., Kuiken, T., Herfst, S., Bestebroer, T., Lamers, M.M., Munnink, B.B.O., De Meulder, D., Van Amerongen, G., Van Den Brand, J., Okba, N.M.A., Schipper, D., Van Run, P., Leijten, L., Sikkema, R., Verschoor, E., Verstrepen, B., Bogers, W., Langermans, J., Langermans, J., Drosten, C., Van Vlissingen, M.F., Fouchier, R., De Swart, R., Koopmans, M., Haagmans, B.L., 2020. Comparative pathogenesis of COVID-19, MERS, and SARS in a nonhuman primate model. Science 368, 1012–1015.

Rolle, A.M., Hasenberg, M., Thornton, C.R., Solouk-Saran, D., Mann, L., Weski, J., Maurer, A., Fischer, E., Spycher, P.R., Schibli, R., Boschetti, F., Stegemann-Koniszewski, S., Bruder, D., Severin, G.W., Autenrieth, S.E., Krappmann, S., Davies, G., Pichler, B.J., Gunzer, M., Wiehr, S., 2016. ImmunoPET/MR imaging allows specific detection of Aspergillus fumigatus lung infection in vivo. Proc Natl Acad Sci U S A 113, E1026–1033.

Santangelo, P.J., Rogers, K.A., Zurla, C., Blanchard, E.L., Gumber, S., Strait, K., Connor-Stroud, F., Schuster, D.M., Amancha, P.K., Hong, J.J., Byrareddy, S.N., Hoxie, J.A., Vidakovic, B., Ansari, A.A., Hunter, E., Villinger, F., 2015. Whole-body immunoPET reveals active SIV dynamics in viremic and antiretroviral therapy-treated macaques. Nat. Methods 12, 427–432.

Sariol, A., Perlman, S., 2020. Lessons for COVID-19 immunity from other coronavirus infections. Immunity 53, 248–263.

Saslaw, S., Wilson, H.E., Doan, C.A., Woolpert, O.C., Schwab, J.L., 1946. Reactions of monkeys to experimentally induced influenza virus a infection : an analysis of the relative roles of humoral and cellular immunity under conditions of optimal or deficient nutrition. J. Exp. Med. 84, 113–125.

Scanga, C.A., Flynn, J.L., 2014. Modeling tuberculosis in nonhuman primates. Cold Spring Harb. Perspect. Med. 4 a018564-a018564.

Schueepp, K.G., Devadason, S.G., Roller, C., Minocchieri, S., Moeller, A., Hamacher, J., Wildhaber, J.H., 2009. Aerosol delivery of nebulised budesonide in young children with asthma. Respir. Med. 103, 1738–1745.

Schuepp, K.G., Jauernig, J., Janssens, H.M., Tiddens, H.A., Straub, D.A., Stangl, R., Keller, M., Wildhaber, J.H., 2005. In vitro determination of the optimal particle size for nebulized aerosol delivery to infants. J. Aerosol Med. 18, 225–235.

Scott, G.H., Stephen, E.L., Berendt, R.F., 1978. Activity of amantadine, rimantadine, and ribavirin against swine influenza in mice and squirrel monkeys. Antimicrob. Agents Chemother. 13, 284–288.

Sesterhenn, F., Yang, C., Bonet, J., Cramer, J.T., Wen, X., Wang, Y., Chiang, C.-I., Abriata, L.A., Kucharska, I., Castoro, G., Vollers, S.S., Galloux, M., Dheilly, E., Rosset, S., Corthésy, P., Georgeon, S., Villard, M., Richard, C.-A., Descamps, D., Delgado, T., Oricchio, E., Rameix-Welti, M.-A., Más, V., Ervin, S., Eléouët, J.-F., Riffault, S., Bates, J.T., Julien, J.-P., Li, Y., Jardetzky, T., Krey, T., Correia, B.E., 2020. De novo protein design enables the precise induction of RSV-neutralizing antibodies. Science 368.

Shan, C., Yao, Y.F., Yang, X.L., Zhou, Y.W., Gao, G., Peng, Y., Yang, L., Hu, X., Xiong, J., Jiang, R.D., Zhang, H.J., Gao, X.X., Peng, C., Min, J., Chen, Y., Si, H.R., Wu, J., Zhou, P., Wang, Y.Y., Wei, H.P., Pang, W., Hu, Z.F., Lv, L.B., Zheng, Y.T., Shi, Z.L., Yuan, Z.M., 2020. Infection with novel coronavirus (SARS-CoV-2) causes pneumonia in Rhesus macaques. Cell Res. 30, 670–677.

Sharpe, S., White, A., Gleeson, F., McIntyre, A., Smyth, D., Clark, S., Sarfas, C., Laddy, D., Rayner, E., Hall, G., Williams, A., Dennis, M., 2016. Ultra low dose aerosol challenge with Mycobacterium tuberculosis leads to divergent outcomes in rhesus and cynomolgus macaques. Tuberculosis 96, 1–12.

Sharpe, S.A., White, A.D., Sibley, L., Gleeson, F., Hall, G.A., Basaraba, R.J., McIntyre, A., Clark, S.O., Gooch, K., Marsh, P.D., Williams, A., Dennis, M.J., 2017. An aerosol challenge model of tuberculosis in Mauritian cynomolgus macaques. PLoS One 12, e0171906.

Shi, T., McAllister, D.A., O'Brien, K.L., Simoes, E.A.F., Madhi, S.A., Gessner, B.D., Polack, F.P., Balsells, E., Acacio, S., Aguayo, C., Alassani, I., Ali, A., Antonio, M., Awasthi, S., Awori, J.O., Azziz-Baumgartner, E., Baggett, H.C., Baillie, V.L., Balmaseda, A., Barahona, A., Basnet, S., Bassat, Q., Basualdo, W., Bigogo, G., Bont, L., Breiman, R.F., Brooks, W.A., Broor, S., Bruce, N., Bruden, D., Buchy, P., Campbell, S., Carosone-Link, P., Chadha, M., Chipeta, J., Chou, M., Clara, W., Cohen, C., de Cuellar, E., Dang, D.-A., Dash-yandag, B., Deloria-Knoll, M., Dherani, M., Eap, T., Ebruke, B.E., Echavarria, M., de Freitas Lázaro Emediato, C.C., Fasce, R.A., Feikin, D.R., Feng, L., Gentile, A., Gordon, A., Goswami, D., Goyet, S., Groome, M., Halasa, N., Hirve, S., Homaira, N., Howie, S.R.C., Jara, J., Jroundi, I., Kartasasmita, C.B., Khuri-Bulos, N., Kotloff, K.L., Krishnan, A., Libster, R., Lopez, O., Lucero, M.G., Lucion, F., Lupisan, S.P., Marcone, D.N., McCracken, J.P., Mejia, M., Moisi, J.C., Montgomery, J.M., Moore, D.P., Moraleda, C., Moyes, J., Munywoki, P., Mutyara, K., Nicol, M.P., Nokes, D.J., Nymadawa, P., da Costa Oliveira, M.T., Oshitani, H., Pandey, N., Paranhos-Baccalà, G., Phillips, L.N., Picot, V.S., Rahman, M., Rakoto-Andrianarivelo, M., Rasmussen, Z.A., Rath, B.A., Robinson, A., Romero, C., Russomando, G., Salimi, V., Sawatwong, P., Scheltema, N., Schweiger, B., Scott, J.A.G., Seidenberg, P., Shen, K., Singleton, R., Sotomayor, V., Strand, T.A., Sutanto, A., Sylla, M., Tapia, M.D., Thamthitiwat, S., Thomas, E.D., Tokarz, R., Turner, C., Venter, M., Waicharoen, S., Wang, J., Watthanaworawit, W., Yoshida, L.-M., Yu, H., Zar, H.J., Campbell, H., Nair, H., 2017. Global, regional, and national disease burden estimates of acute lower respiratory infections due to respiratory syncytial virus in young children in 2015: a systematic review and modelling study. Lancet 390.

Shi, J., Wen, Z., Zhong, G., Yang, H., Wang, C., Huang, B., Liu, R., He, X., Shuai, L., Sun, Z., Zhao, Y., Liu, P., Liang, L., Cui, P., Wang, J., Zhang, X., Guan, Y., Tan, W.,

Wu, G., Chen, H., Bu, Z., Bu, Z., 2020. Susceptibility of ferrets, cats, dogs, and other domesticated animals to SARS-coronavirus 2. Science 368, 1016–1020.

Shie, J.J., Fang, J.M., 2019. Development of effective anti-influenza drugs: congeners and conjugates - a review. J. Biomed. Sci. 26, 84.

Sia, S.F., Yan, L.M., Chin, A.W.H., Fung, K., Choy, K.T., Wong, A.Y.L., Kaewpreedee, P., Perera, R.A.P.M., Poon, L.L.M., Nicholls, J.M., Peiris, M., Yen, H.L., 2020. Pathogenesis and transmission of SARS-CoV-2 in golden hamsters. Nature 583, 834–838.

Sibley, L., Dennis, M., Sarfas, C., White, A., Clark, S., Gleeson, F., McIntyre, A., Rayner, E., Pearson, G., Williams, A., Marsh, P., Sharpe, S., 2016. Route of delivery to the airway influences the distribution of pulmonary disease but not the outcome of Mycobacterium tuberculosis infection in rhesus macaques. Tuberculosis 96, 141–149.

Simoes, E.A.F., Hayward, A.R., Ponnuraj, E.M., Straumanis, J.P., Stenmark, K.R., Wilson, H.L., Babu, P.G., 1999. Respiratory syncytial virus infects the bonnet monkey, <i>Macaca radiata</i>. Pediatr. Dev. Pathol. 2.

Simonsen, L., Clarke, M.J., Schonberger, L.B., Arden, N.H., Cox, N.J., Fukuda, K., 1998. Pandemic versus epidemic influenza mortality: a pattern of changing age distribution. J. Infect. Dis. 178, 53–60.

Singh, D.K., Singh, B., Ganatra, S.R., Gazi, M., Cole, J., Thippeshappa, R., Alfson, K.J., Clemmons, E., Gonzalez, O., Escobedo, R., Lee, T.H., Chatterjee, A., Goez-Gazi, Y., Sharan, R., Gough, M., Alvarez, C., Blakley, A., Ferdin, J., Bartley, C., Staples, H., Parodi, L., Callery, J., Mannino, A., Klaffke, B., Escareno, P., Platt, R.N., Hodara, V., Scordo, J., Gautam, S., Vilanova, A.G., Olmo-Fontanez, A., Schami, A., Oyejide, A., Ajithdoss, D.K., Copin, R., Baum, A., Kyratsous, C., Alvarez, X., Ahmed, M., Rosa, B., Goodroe, A., Dutton, J., Hall-Ursone, S., Frost, P.A., Voges, A.K., Ross, C.N., Sayers, K., Chen, C., Hallam, C., Khader, S.A., Mitreva, M., Anderson, T.J.C., Martinez-Sobrido, L., Patterson, J.L., Turner, J., Torrelles, J.B., Dick, E.J., Brasky, K., Schlesinger, L.S., Giavedoni, L.D., Carrion, R., Kaushal, D., 2021. Responses to acute infection with SARS-CoV-2 in the lungs of rhesus macaques, baboons and marmosets. Nat. Microbiol. 6, 73–86.

Singleton, R., Etchart, N., Hou, S., Hyland, L., 2003. Inability to evoke a long-lasting protective immune response to respiratory syncytial virus infection in mice correlates with ineffective nasal antibody responses. J. Virol. 77, 11303–11311.

Sloan, E.K., Capitanio, J.P., Tarara, R.P., Mendoza, S.P., Mason, W.A., Cole, S.W., 2007. Social stress enhances sympathetic innervation of primate lymph nodes: mechanisms and implications for viral pathogenesis. J. Neurosci. 27, 8857–8865.

Slomka, P.J., Pan, T., Germano, G., 2016. Recent advances and future progress in PET instrumentation. Semin. Nucl. Med. 46, 5–19.

Smits, S.L., de Lang, A., van den Brand, J.M.A., Leijten, L.M., van Ijcken, W.F., Eijkemans, M.J.C., van Amerongen, G., Kuiken, T., Andeweg, A.C., Osterhaus, A.D. M.E., Haagmans, B.L., 2010. Exacerbated innate host response to SARS-CoV in aged non-human Primates. PLoS Pathog. 6, e1000756.

Standardization, E.Cf., 2007. Respiratory Therapy Equipment - Part 1: Nebulizing Systems and Their Components. CEN.

Stark, J.M., McDowell, S.A., Koenigsknecht, V., Prows, D.R., Leikauf, J.E., Le Vine, A.M., Leikauf, G.D., 2002. Genetic susceptibility to respiratory syncytial virus infection in inbred mice. J. Med. Virol. 67.

Stephen, E.L., Walker, J.S., Dominik, J.W., Young, H.W., Berendt, R.F., 1977. Aerosol therapy of influenza infections of mice and primates with rimantadine, ribavirin, and related compounds. Ann. N. Y. Acad. Sci. 284, 264–271.

Stittelaar, K., de Waal, L., van Amerongen, G., Veldhuis Kroeze, E., Fraaij, P., van Baalen, C., van Kampen, J., van der Vries, E., Osterhaus, A., de Swart, R., 2016. Ferrets as a novel animal model for studying human respiratory syncytial virus infections in Immunocompetent and immunocompromised hosts. Viruses 8.

Sun, S.H., Chen, Q., Gu, H.J., Yang, G., Wang, Y.X., Huang, X.Y., Liu, S.S., Zhang, N.N., Li, X.F., Xiong, R., Guo, Y., Deng, Y.Q., Huang, W.J., Liu, Q., Liu, Q.M., Shen, Y.L., Zhou, Y., Yang, X., Zhao, T.Y., Fan, C.F., Zhou, Y.S., Qin, C.F., Wang, Y.C., 2020. A mouse model of SARS-CoV-2 infection and pathogenesis. Cell Host Microbe 28, 124–133 e124.

Szentiks, C.A., Köndgen, S., Silinski, S., Speck, S., Leendertz, F.H., 2009. Lethal pneumonia in a captive juvenile chimpanzee (<i>Pan troglodytes</i>) due to human-transmitted human respiratory syncytial virus (HRSV) and infection with <i>Streptococcus pneumoniae</i>. J. Med. Primatol. 38.

Taylor, G., 2017. Animal models of respiratory syncytial virus infection. Vaccine 35.

Teng, M.N., Whitehead, S.S., Bermingham, A., St. Claire, M., Elkins, W.R., Murphy, B.R., Collins, P.L., 2000. Recombinant respiratory syncytial virus that does not express the NS1 or M2-2 protein is highly attenuated and immunogenic in chimpanzees. J. Virol. 74.

Thiberville, L., Moreno-Swirc, S., Vercauteren, T., Peltier, E., Cavé, C., Bourg Heckly, G., 2007. In vivo imaging of the bronchial wall microstructure using fibered confocal fluorescence microscopy. Am. J. Respir. Crit. Care Med. 175, 22–31.

Thiberville, L., Salaün, M., Lachkar, S., Dominique, S., Moreno-Swirc, S., Vever-Bizet, C., Bourg-Heckly, G., 2009. Human in vivo fluorescence microimaging of the alveolar ducts and sacs during bronchoscopy. Eur. Respir. J. 33, 974–985.

Thomas, R.J., 2013. Particle size and pathogenicity in the respiratory tract. Virulence 4.

Thompson, W.W., Shay, D.K., Weintraub, E., Brammer, L., Cox, N., Anderson, L.J., Fukuda, K., 2003. Mortality associated with influenza and respiratory syncytial virus in the United States. JAMA 289, 179–186.

Thornhill, E.M., Salpor, J., Verhoeven, D., 2020. Respiratory syntycial virus: current treatment strategies and vaccine approaches. Antivir. Chem. Chemother. 28.

Thornton, C.R., 2018. Molecular imaging of invasive pulmonary aspergillosis using ImmunoPET/MRI: the future looks bright. Front. Microbiol. 9, 691.

Tian, J.-H., Patel, N., Haupt, R., Zhou, H., Weston, S., Hammond, H., Logue, J., Portnoff, A.D., Norton, J., Guebre-Xabier, M., Zhou, B., Jacobson, K., Maciejewski, S., Khatoon, R., Wisniewska, M., Moffitt, W., Kluepfel-Stahl, S.,

Ekechukwu, B., Papin, J., Boddapati, S., Jason Wong, C., Piedra, P.A., Frieman, M.B., Massare, M.J., Fries, L., Bengtsson, K.L., Stertman, L., Ellingsworth, L., Glenn, G., Smith, G., 2021. SARS-CoV-2 spike glycoprotein vaccine candidate NVX-CoV2373 immunogenicity in baboons and protection in mice. Nat. Commun. 12.

Trevejo-Nunez, G., Chen, K., Dufour, J.P., Bagby, G.J., Horne, W.T., Nelson, S., Kolls, J. K., 2015. Ethanol impairs mucosal immunity against Streptococcus pneumoniae infection by disrupting interleukin 17 gene expression. Infect. Immun. 83, 2082–2088.

Tseng, C.-T.K., Huang, C., Newman, P., Wang, N., Narayanan, K., Watts, D.M., Makino, S., Packard, M.M., Zaki, S.R., Chan, T.-s., Peters, C.J., 2007. Severe acute respiratory syndrome coronavirus infection of mice transgenic for the human angiotensin-converting enzyme 2 virus receptor. J. Virol. 81, 1162–1173.

Van Andel, R., Sherwood, R., Gennings, C., Lyons, C.R., Hutt, J., Gigliotti, A., Barr, E., 2008. Clinical and pathologic features of cynomolgus macaques (Macaca fascicularis) infected with aerosolized Yersinia pestis. Comp. Med. 58, 68–75.

van den Brand, J.M., Haagmans, B.L., van Riel, D., Osterhaus, A.D., Kuiken, T., 2014. The pathology and pathogenesis of experimental severe acute respiratory syndrome and influenza in animal models. J. Comp. Pathol. 151, 83–112.

van der Hoek, L., Pyrc, K., Jebbink, M.F., Vermeulen-Oost, W., Berkhout, R.J.M., Wolthers, K.C., Wertheim-van Dillen, P.M.E., Kaandorp, J., Spaargaren, J., Berkhout, B., 2004. Identification of a new human coronavirus. Nat. Med. 10, 368–373.

Van Kerkhove, M.D., Hirve, S., Koukounari, A., Mounts, A.W., group, H.N.p.s.w, 2013. Estimating age-specific cumulative incidence for the 2009 influenza pandemic: a meta-analysis of A(H1N1)pdm09 serological studies from 19 countries. Influenza Other Respir. Viruses 7, 872–886.

Vasconcelos, D., Barnewall, R., Babin, M., Hunt, R., Estep, J., Nielsen, C., Carnes, R., Carney, J., 2003. Pathology of inhalation anthrax in cynomolgus monkeys (Macaca fascicularis). Lab. Invest. 83, 1201–1209.

Via, L.E., Weiner, D.M., Schimel, D., Lin, P.L., Dayao, E., Tankersley, S.L., Cai, Y., Coleman, M.T., Tomko, J., Paripati, P., Orandle, M., Kastenmayer, R.J., Tartakovsky, M., Rosenthal, A., Portevin, D., Eum, S.Y., Lahouar, S., Gagneux, S., Young, D.B., Flynn, J.L., Barry, C.E., 2013. Differential virulence and disease progression following Mycobacterium tuberculosis complex infection of the common marmoset (Callithrix jacchus). Infect. Immun. 81.

Wang, M., Lamberth, K., Harndahl, M., Roder, G., Stryhn, A., Larsen, M.V., Nielsen, M., Lundegaard, C., Tang, S.T., Dziegiel, M.H., Rosenkvist, J., Pedersen, A.E., Buus, S., Claesson, M.H., Lund, O., 2007. CTL epitopes for influenza A including the H5N1 bird flu; genome-, pathogen-, and HLA-wide screening. Vaccine 25, 2823–2831.

Wang, D., Cummins, C., Bayliss, S., Sandercock, J., Burls, A., 2008. Immunoprophylaxis against respiratory syncytial virus (RSV) with palivizumab in children: a systematic review and economic evaluation. Health Technol. Assess. (Rockv) 12.

Warfel, J.M., Beren, J., Kelly, V.K., Lee, G., Merkel, T.J., 2012a. Nonhuman primate model of pertussis. Infect. Immun. 80, 1530–1536.

Warfel, J.M., Beren, J., Merkel, T.J., 2012b. Airborne transmission of Bordetella pertussis. J. Infect. Dis. 206, 902–906.

Warfel, J.M., Beren, J., Merkel, T.J., 2012c. Airborne transmission of Bordetella pertussis. J. Infect. Dis. 206.

Warfel, J.M., Papin, J.F., Wolf, R.F., Zimmerman, L.I., Merkel, T.J., 2014a. Maternal and neonatal vaccination protects newborn baboons from pertussis infection. J. Infect. Dis. 210, 604–610.

Warfel, J.M., Zimmerman, L.I., Merkel, T.J., 2014b. Acellular pertussis vaccines protect against disease but fail to prevent infection and transmission in a nonhuman primate model. Proc. Natl. Acad. Sci. U.S.A. 111, 787–792.

Warfel, J.M., Zimmerman, L.I., Merkel, T.J., 2016. Comparison of three whole-cell pertussis vaccines in the baboon model of pertussis. Clin. Vaccine Immunol. 23, 47–54.

Watanabe, T., Iwatsuki-Horimoto, K., Kiso, M., Nakajima, N., Takahashi, K., Jose da Silva Lopes, T., Ito, M., Fukuyama, S., Hasegawa, H., Kawaoka, Y., 2018. Experimental infection of Cynomolgus macaques with highly pathogenic H5N1 influenza virus through the aerosol route. Sci. Rep. 8.

Weinstein, E.A., Ordonez, A.A., DeMarco, V.P., Murawski, A.M., Pokkali, S., MacDonald, E.M., Klunk, M., Mease, R.C., Pomper, M.G., Jain, S.K., 2014. Imaging Enterobacteriaceae infection in vivo with 18F-fluorodeoxysorbitol positron emission tomography. Sci. Transl. Med. 6, 259ra146.

Weltzin, R., Traina-Dorge, V., Soike, K., Zhang, J.Y., Mack, P., Soman, G., Drabik, G., Monath, T.P., 1996. Intranasal monoclonal IgA antibody to respiratory syncytial virus protects Rhesus monkeys against upper and lower respiratory tract infection. J. Infect. Dis. 174.

WHO, 2018a. Influenza (Avian and Other Zoonotic). WHO, pp. 1–7. https://www.who. int/news-room/fact-sheets/detail/influenza-(avian-and-other-zoonotic).

WHO, 2018b. WHO | Diphtheria-tetanus-pertussis (DTP3) Immunization Coverage.

WHO, 2020. Global Tuberculosis Report 2020.

WHO, 2021. WHO Coronavirus Disease (COVID-19) Dashboard. Who.int.

Widmer, K., Zhu, Y., Williams, J.V., Griffin, M.R., Edwards, K.M., Talbot, H.K., 2012. Rates of hospitalizations for respiratory syncytial virus, human metapneumovirus, and influenza virus in older adults. J. Infect. Dis. 206.

Wiehr, S., Warnke, P., Rolle, A.-M., Schütz, M., Oberhettinger, P., Kohlhofer, U., Quintanilla-Martinez, L., Maurer, A., Thornton, C., Boschetti, F., Reischl, G., Autenrieth, I.B., Pichler, B.J., Autenrieth, S.E., 2016. New pathogen-specific immunoPET/MR tracer for molecular imaging of a systemic bacterial infection. Oncotarget 7, 10990–11001.

Williamson, B.N., Feldmann, F., Schwarz, B., Meade-White, K., Porter, D.P., Schulz, J., van Doremalen, N., Leighton, I., Yinda, C.K., Pérez-Pérez, L., Okumura, A., Lovaglio, J., Hanley, P.W., Saturday, G., Bosio, C.M., Anzick, S., Barbian, K., Cihlar, T., Martens, C., Scott, D.P., Munster, V.J., de Wit, E., 2020. Clinical benefit of remdesivir in rhesus macaques infected with SARS-CoV-2. Nature 585, 273–276.

Wolff, R.K., 1996. Experimental investigation of deposition and fate of particles: animal models and interspecies differences. In: Marijnissen, J.C.M., Gradoń, L. (Eds.), Aerosol Inhalation: Recent Research Frontiers: Proceedings of the International Workshop on Aerosol Inhalation, Lung Transport, Deposition and the Relation to the Environment: Recent Research Frontiers. Warsaw, Poland, September 14–16, 1995. Springer Netherlands, Dordrecht, pp. 247–263.

Wonderlich, E.R., Swan, Z.D., Bissel, S.J., Hartman, A.L., Carney, J.P., O'Malley, K.J., Obadan, A.O., Santos, J., Walker, R., Sturgeon, T.J., Frye Jr., L.J., Maiello, P., Scanga, C.A., Bowling, J.D., Bouwer, A.L., Duangkhae, P.A., Wiley, C.A., Flynn, J.L., Wang, J., Cole, K.S., Perez, D.R., Reed, D.S., Barratt-Boyes, S.M., 2017. Widespread virus replication in alveoli drives acute respiratory distress syndrome in aerosolized H5N1 influenza infection of macaques. J. Immunol. 198, 1616–1626.

Wong, B.A., 2007. Inhalation exposure systems: design, methods and operation. Toxicol. Pathol. 35.

Woo, P.C.Y., Lau, S.K.P., Chu, C.-m., Chan, K.-h., Tsoi, H.-w., Huang, Y., Wong, B.H.L., Poon, R.W.S., Cai, J.J., Luk, W.-k., Poon, L.L.M., Wong, S.S.Y., Guan, Y., Peiris, J.S. M., Yuen, K.-y., 2005. Characterization and complete genome sequence of a novel coronavirus, coronavirus HKU1, from patients with pneumonia. J. Virol. 79, 884–895.

Woolsey, C., Borisevich, V., Prasad, A.N., Agans, K.N., Deer, D.J., Dobias, N.S., Heymann, J.C., Foster, S.L., Levine, C.B., Medina, L., Melody, K., Geisbert, J.B., Fenton, K.A., Geisbert, T.W., Cross, R.W., 2021. Establishment of an African green monkey model for COVID-19 and protection against re-infection. Nat. Immunol. 22.

Yao, Y., Bao, L., Deng, W., Xu, L., Li, F., Lv, Q., Yu, P., Chen, T., Xu, Y., Zhu, H., Yuan, J., Gu, S., Wei, Q., Chen, H., Yuen, K.Y., Qin, C., 2014. An animal model of mers produced by infection of rhesus macaques with MERS coronavirus. J. Infect. Dis. 209, 236–242.

Yeh, H.C., Brinker, R.M., Harkema, J.R., Muggenburg, B.A., 1997. A comparative analysis of primate nasal airways using magnetic resonance imaging and nasal casts. J. Aerosol Med. 10.

Yu, H., Gao, Z., Feng, Z., Shu, Y., Xiang, N., Zhou, L., Huai, Y., Feng, L., Peng, Z., Li, Z., Xu, C., Li, J., Hu, C., Li, Q., Xu, X., Liu, X., Liu, Z., Xu, L., Chen, Y., Luo, H., Wei, L., Zhang, X., Xin, J., Guo, J., Wang, Q., Yuan, Z., Zhou, L., Zhang, K., Zhang, W., Yang, J., Zhong, X., Xia, S., Li, L., Cheng, J., Ma, E., He, P., Lee, S.S., Wang, Y., Uyeki, T.M., Yang, W., 2008. Clinical characteristics of 26 human cases of highly pathogenic avian influenza A (H5N1) virus infection in China. PLoS One 3, e2985.

Yu, P., Qi, F., Xu, Y., Li, F., Liu, P., Liu, J., Bao, L., Deng, W., Gao, H., Xiang, Z., Xiao, C., Lv, Q., Gong, S., Liu, J., Song, Z., Qu, Y., Xue, J., Wei, Q., Liu, M., Wang, G., Wang, S., Yu, H., Liu, X., Huang, B., Wang, W., Zhao, L., Wang, H., Ye, F., Zhou, W., Zhen, W., Han, J., Wu, G., Jin, Q., Wang, J., Tan, W., Qin, C., 2020. Age-related rhesus macaque models of COVID-19. Anim. Model. Exp. Med. 3, 93–97.

Zaki, A.M., van Boheemen, S., Bestebroer, T.M., Osterhaus, A.D.M.E., Fouchier, R.A.M., 2012. Isolation of a novel coronavirus from a man with pneumonia in Saudi Arabia. N. Engl. J. Med. 367, 1814–1820.

Zaucha, G.M., Jahrling, P.B., Geisbert, T.W., Swearengen, J.R., Hensley, L., 2001. The pathology of experimental aerosolized monkeypox virus infection in cynomolgus monkeys (Macaca fascicularis). Lab. Invest. 81, 1581–1600.

Zhao, J., Li, K., Wohlford-Lenane, C., Agnihothram, S.S., Fett, C., Zhao, J., Gale, M.J., Baric, R.S., Enjuanes, L., Gallagher, T., McCray, P.B., Perlman, S., 2014. Rapid generation of a mouse model for Middle East respiratory syndrome. Proc. Natl. Acad. Sci. U.S.A. 111, 4970–4975.

Zhao, J.J., Zhao, J.J., Mangalam, A.K., Channappanavar, R., Fett, C., Meyerholz, D.K., Agnihothram, S., Baric, R.S., David, C.S., Perlman, S., 2016. Airway memory CD4+ t cells mediate protective immunity against emerging respiratory coronaviruses. Immunity 44, 1379–1391.

Zhou, P., Yang, X.L., Wang, X.G., Hu, B., Zhang, L., Zhang, W., Si, H.R., Zhu, Y., Li, B., Huang, C.L., Chen, H.D., Chen, J., Luo, Y., Guo, H., Jiang, R.D., Liu, M.Q., Chen, Y., Shen, X.R., Wang, X., Zheng, X.S., Zhao, K., Chen, Q.J., Deng, F., Liu, L.L., Yan, B., Zhan, F.X., Wang, Y.Y., Xiao, G.F., Shi, Z.L., 2020. A pneumonia outbreak associated with a new coronavirus of probable bat origin. Nature 579, 270–273.